Australian Government
Geoscience Australia

Investigation of drill holes in the vicinity of the 08GA-C1 seismic line in the Curnamona Province, South Australia

Anthony Schofield

Record
2010/21

GeoCat # 70495

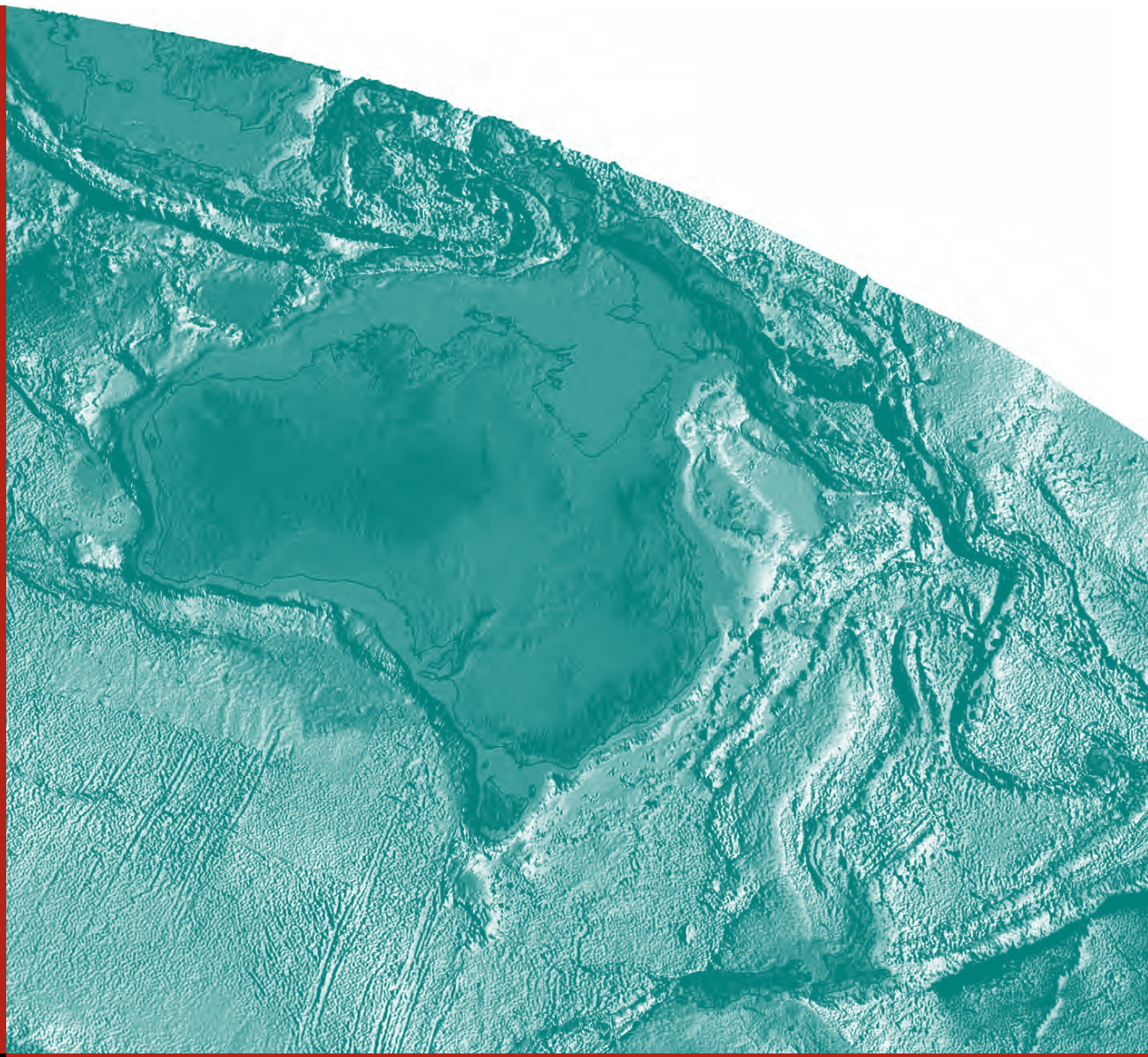

Investigation of drill holes in the vicinity of the 08GA-C1 seismic line in the Curnamona Province, South Australia

GEOSCIENCE AUSTRALIA
RECORD 2010/21

by

Anthony Schofield[1]

Australian Government
Geoscience Australia

1. Onshore Energy and Minerals Division, Geoscience Australia

Department of Resources, Energy and Tourism
Minister for Resources and Energy: The Hon. Martin Ferguson, AM MP
Secretary: Mr Drew Clarke

Geoscience Australia
Chief Executive Officer: Dr Chris Pigram

ISSN 1448-2177
ISBN 978-1-921781-07-0 print
ISBN 978-1-921781-08-7 web

GeoCat # 70495

Bibliographic reference: Schofield, A., 2010. Investigation of drill holes in the vicinity of the 08GA-C1 seismic line in the Curnamona Province, South Australia. Geoscience Australia Record, 2010/21, 33p.

Contents

Executive Summary

The Curnamona Province in eastern South Australia is host to significant mineral and energy resources, including uranium, copper-gold and geothermal resources. The Province is largely buried beneath recent sediments, with outcrop restricted to the Olary and Broken Hill Domains in the south, and the Mount Painter region in the north. In order to understand the subsurface geology in the Curnamona Province, several deep crustal seismic reflection surveys have been undertaken. Most recently, the 08GA-C1 seismic line was acquired as part of Geoscience Australia's Onshore Energy Security Program. This line extends from the previously acquired 03GA-CU1 line in the south, and runs north to the Mount Painter area through the Benagerie Ridge.

The prevalence of recent sediments in the area covered by the seismic line renders it difficult to constrain the geology imaged by the seismic data. To assist regional geological interpretation, seven widely spaced drill holes in the vicinity of the seismic line have been investigated. These drill holes intersect both sedimentary and igneous units which have been sampled for geochemical, geochronological and petrographic studies. The results of these studies and pertinent existing data are summarised in this report.

Key findings of this investigation are:

- A new A-type granite has been identified and dated at ~1590 Ma. This is similar in age to the A-type Benagerie Volcanics, which together may represent a volcanic-plutonic association analogous to the similarly aged Hiltaba Suite-Gawler Range Volcanics association observed in the Gawler Craton.
- The alteration assemblage and paragenesis in highly altered rocks intersected in BWM1A-1 and ETM5A-1 is similar to that typical of iron oxide-copper-gold mineral systems. This, together with the known presence of A-type magmatism, confirms the previously recognised potential of the Curnamona Province for iron oxide-copper-gold mineralisation.
- The stratigraphy intersected in Bumbarlow 1 may be divided into four broad packages. New detrital zircon dating permits a possible correlation with the Pandurra Formation. Basic volcanics in Bumbarlow 1 are similar to Benagerie Volcanics intersected in LNM10. These in turn have been linked to felsic volcanics encountered elsewhere on the Benagerie Ridge which are contemporary with the voluminous Gawler Range Volcanics in the Gawler Craton to the west. The volcanics in Bumbarlow 1 probably represent a mafic equivalent of the Gawler Range Volcanics.
- Calc-silicate rocks with anomalous zinc contents intersected in SPH1 had an igneous protolith of comparable age to granitoids in the Mount Painter region.

Introduction

The Proterozoic Curnamona Province is a largely buried crustal block spanning the South Australia-New South Wales border and covering an area of approximately 80,000 km^2. Outcropping geology is mostly restricted to the southern Curnamona Province, and is dominated by the Paleoproterozoic Willyama Supergroup (Conor and Preiss, 2008). Magmatism occurred in three main phases in the Curnamona Province between ~1715 and 1580 Ma (Conor and Preiss, 2008), and includes episodes of A- and S-type magmatism.

Although best known for the Broken Hill Pb-Zn deposit in the Broken Hill Domain, the Province also hosts significant U mineralisation in both basement granites (eg., the Crocker Well group of deposits in the southern Curnamona Province; Wilson and Fairclough, 2009), and in younger palaeochannels (eg., Skirrow, 2009). The Province is thought to have high potential for iron oxide-copper-gold (IOCG) deposits, with a number of Cu-Au prospects showing IOCG affinities (Skirrow and Ashley, 2000; Teale, 2000). As well as significant mineral potential, the Curnamona Province hosts high heat producing granites and is partially included within the South Australian Heat Flow Anomaly (Neumann et al., 2000). This, in conjunction with the widespread insulating sedimentary cover, suggests considerable geothermal energy potential.

As part of the Onshore Energy Security Program, Geoscience Australia has acquired a ~262 km long deep crustal seismic reflection line (08GA-C1; Korsch et al., 2010) running north-south through the central Curnamona Province (Fig. 1). The southern extent of the line links with previously acquired seismic data (03GA-CU1; Goleby et al., 2006), which itself is linked with other seismic lines (Gibson et al., 1998) to provide a comprehensive image of the crustal structure in the Curnamona Province. Together, these data allow for the crustal architecture and geodynamic evolution of the Curnamona Province to be better understood. This enhanced geological understanding will inform the understanding of the mineral and energy potential of the Province.

To help constrain the geology imaged by the seismic survey, seven drill holes were investigated along 08GA-C1 (Fig. 1). These provide geological context and characterise the packages imaged by the seismic data. This report describes the petrographic, geochemical and geochronological studies conducted on samples from these drill holes. It will seek to describe and characterise the geology intersected, and summarise arising implications for mineral systems in the Curnamona Province.

Methods

A total of seven holes were inspected and sampled for geochemical or geochronological analysis: BRD012, BRD013, SPH1, ETM5A-1, BWM1A-1, LNM10 and Bumbarlow 1. These holes were selected on the basis of their spatial relationship to the 08GA-C1 seismic line and to address relevant geological questions. With the exception of BRD012 and BRD013, all holes were examined at the PIRSA drill core storage facility at Glenside, Adelaide. BRD012 and BRD013 were made available courtesy of Newcrest Mining Limited.

Major and trace element analyses were performed on 34 samples at Geoscience Australia using a Phillips PW2404 XRF spectrometer following the methods of Norrish and Chappell (1977) and an Agilent Technologies 7500 ICP-MS following the methods of Jenner et al. (1990) and Pyke (2000). Iron is reported at total Fe_2O_3, with FeO determined by titration. These data are presented in Appendix 1. Geochronological analysis was performed at Geoscience Australia using a Sensitive High Resolution Ion MicroProbe (SHRIMP) on five samples (2009378001, 2009378006,

2009378018, 2009378027 and 2009378038). For a full description of analytical methodologies, see Fraser and Neumann (2010).

Throughout this report, geochemical data are normalised to post-Archean average Australian sediment (PAAS; McLennan, 1989), N-type mid-ocean ridge basalt (N-MORB; Sun and McDonough, 1989) and the C1 chondrite (Sun and McDonough, 1989).

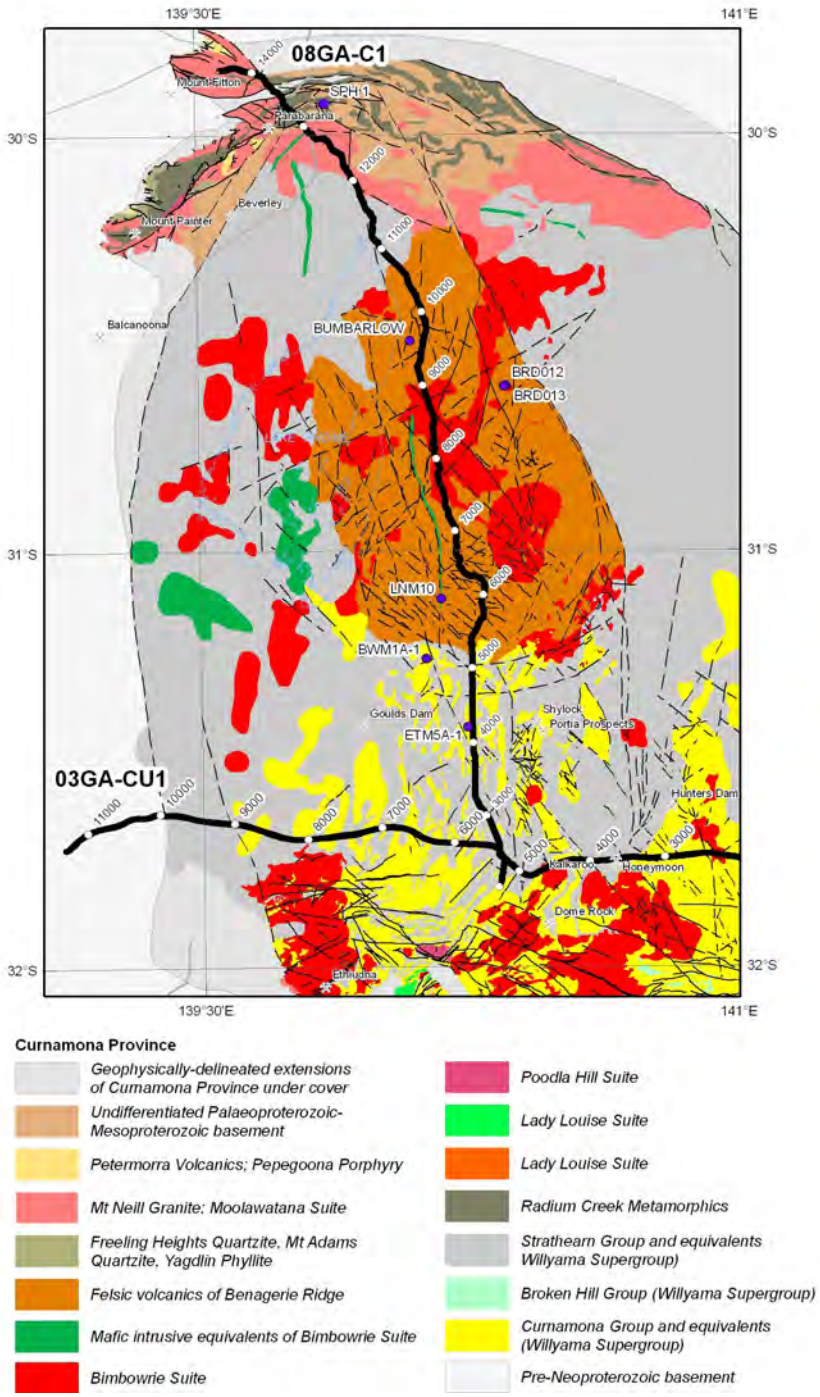

Figure 1: *Location of the 08GA-C1 seismic line and drill holes sampled in this investigation. The 03GA-CU1 seismic line, CDP stations, and the solid geology of Cowley (2006) are also shown.*

Bumbarlow 1

Bumbarlow 1 was drilled in 1978 as a stratigraphic hole to constrain interpretation along Crusader Oil's CFK seismic line (Youngs, 1978). It is situated just east of the northern extent of Lake Frome, and reached a depth of 720.33 m. The hole occurs 4 km west of Geoscience Australia's 08GA-C1 seismic line (Korsch et al., 2010), and therefore provides important information on the geology imaged in the vicinity of the drill hole. Several samples were taken from Bumbarlow 1 to undertake geochemical and geochronological studies to aid in the interpretation of 08GA-C1.

GEOLOGICAL DESCRIPTION

Bumbarlow 1 may be subdivided into four broad packages. These are, from the top of logged section to the bottom of hole: a Cenozoic to Mesozoic sedimentary package, an upper sediments package, a sedimentary and volcanics package, and a basal shale (Fig. 2).

'Cenozoic to Mesozoic package'

The Cenozoic to Mesozoic section extends to ~409 m depth, and has been logged as sedimentary rocks of the Coonarbine Formation, Eurinilla Formation, Namba Formation, Eyre Formation, Marree Subgroup and Cadna-owie Formation (Youngs, 1978). The hole is cored from the base of the Cenozoic-Mesozoic package.

'Upper sediments package'

The 'upper sediments package' is approximately 100 m thick and extends to ~509 m depth. It consists of dominantly reddish-maroon clastic sedimentary rocks, with finer horizons showing green staining in places. The 'upper sediments package' is lithologically similar to the Pandurra Formation (Teale and Flint, 1995), and is mapped as potential Pandurra Formation in the solid geology of South Australia (Cowley, 2006).

The dominant lithology is medium to coarse sandstone, with lesser intervals of siltstone/mudstone and conglomerate. Grains within the sandstone units are moderately to poorly sorted and are angular to subrounded. At around 450 m, the sandstones are predominately quartzose, with lesser feldspar and lithic components. Lithic clasts may be derived from volcanics or underlying metasediments. Quartz shows evidence of recrystallisation, with seriate boundaries between adjacent grains. Feldspar content increases towards the base of the 'upper sediments package'. Sedimentary structures, including cross-bedding, graded bedding and channelling, are evident between 467-491 m. The sandstones are immature, and have been interpreted as being deposited in a fluviatile environment (Teale and Flint, 1995). Finer grained packages occur at 491-500 and 460 m, and are interbedded with sandstone between 409-421 m. Other minor fine horizons are distributed throughout the package. Conglomeratic intervals are common throughout the package, and often show sharp contacts with adjacent finer sediments.

'Sediments and volcanics package'

A package of interbedded clastic sediments and basic volcanics occurs between 509-702 m, and immediately underlies a ~5.5 m thick conglomerate interval which contains clasts of the underlying volcanics (Fig. 3). The clastic sediments consist of upward-fining sandstones, siltstone/mudstone and minor conglomerate. Sandstone units are generally moderately sorted, subangular to subrounded, grain supported, and show reddish hematite staining. Feldspar content is generally high. The

sandstone layer immediately above the 'basal shale' unconformity differs from other sandstone units in the section, being quartz-dominated and white in appearance (due to bleaching?). This lowermost sandstone of the package also contains abundant lithic fragments, some of which resemble pink volcanics. Grading and cross-bedding is observed in many of the sandstone intervals, and channel structures are present at around 579 m. Fine-grained beds are often laminated, and contain minor silty horizons.

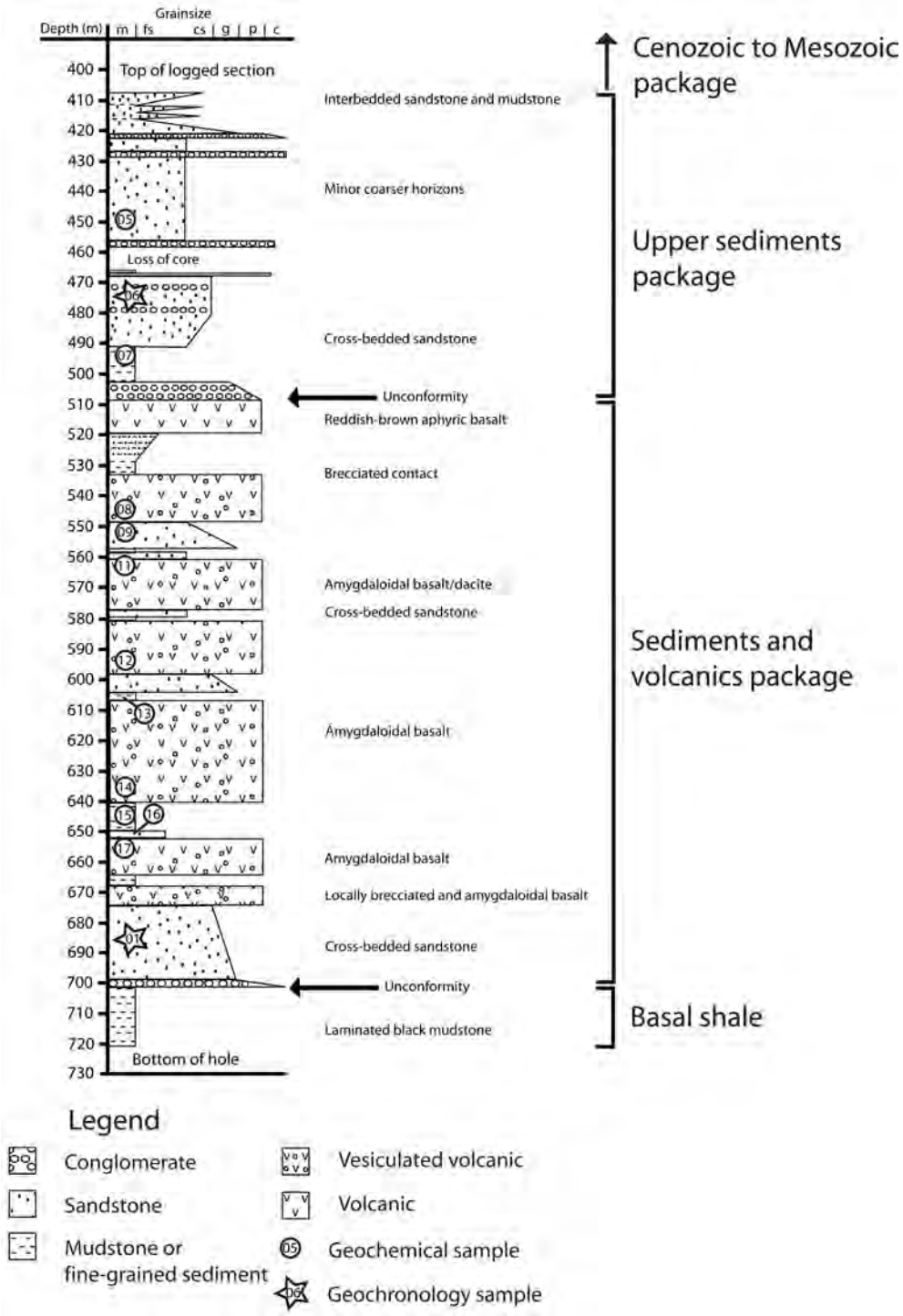

Figure 2: *Geological log of Bumbarlow 1. Sample locations are also shown.*

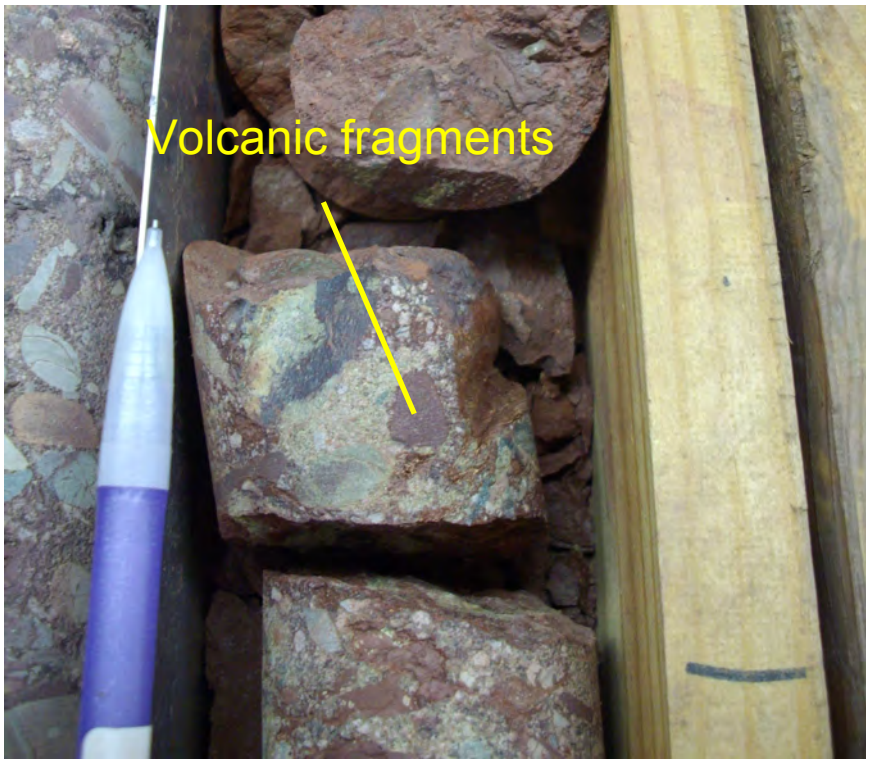

Figure 3: *Photograph of drill core from Bumbarlow 1. Photo taken at the contact between the 'upper sediments package' and the interbedded 'sediments and volcanics package'.*

The volcanics interbedded with the clastic sediments are mafic and appear reddish-brown in hand sample. They are generally highly altered. Individual volcanic horizons are typically 15-20 m thick, locally reaching 33 m. All except the uppermost volcanic interval are amygdaloidal. Amygdales are infilled by quartz, chlorite and calcite, and increase in abundance towards the top of any given volcanic interval. This latter feature suggests that these volcanics were emplaced as lava flows. Thin section analysis of the freshest sample (from 595 m) reveals very fine grained textures with prominent microphenocrystic plagioclase laths and needles. Primary mafic mineralogy is obliterated by secondary chlorite, but probably included clinopyroxene (Giles and Teale, 1981). There are numerous brecciated horizons within the volcanics. Giles and Teale (1981) consider the volcanics in Bumbarlow 1 to be post-orogenic.

'Basal shale'

The 'basal shale' is markedly different in character from the overlying packages. It is described by Youngs (1978) as a dark grey-black laminated shale, dolomitic in bands, and with a 30-40^{o} cleavage in places. There is a prominent unconformity between the shale and the overlying 'sediments and volcanics package'. The shale has been interpreted to belong to the Willyama Supergroup (Robertson et al., 1998).

GEOCHEMISTRY

Fifteen geochemical samples from Bumbarlow 1 were analysed. These data are presented in Appendix 1.

Sedimentary rocks

Samples from the 'upper sediments package' and the 'sediments and volcanics package' were analysed to assess whether different provenances can be identified by the geochemistry. The REE content of sedimentary rocks is predominately controlled by provenance, and is resistant to weathering and alteration (Fleet, 1984; McLennan, 1989; Rollinson, 1993). As such, they are a useful tool for determining shifts in provenance for a sedimentary package.

Two samples taken from the 'sediments and volcanics package' (2009137013 and 2009378015) plot together on normalised REE diagrams, indicating no significant change in source between the thick volcanic unit which occurs between 607 and 641 m. Mudstone taken from the 'upper sediments package' (2009378007) shows deviation from the lower mudstones (Fig. 4). Rare earth element abundances are consistently higher than for the 'sediments and volcanics package'. This effect is especially pronounced in the HREE, with the upper mudstone showing a slightly enriched HREE compared to MREE (Gd_N/Yb_N = 0.91, normalised to PAAS). Another notable feature is a slight Eu anomaly in the 'upper sediments package' (Eu_N/Eu_N^* = 0.81) when normalised to PAAS, while the Eu anomaly in the lower 'sediments and volcanics package' is negligible (Eu_N/Eu_N^* = 0.93-0.97). This suggests a shift in sediment provenance between the sampled mudstone in the upper package compared with that in the lower package.

PAAS-normalised REE patterns are flat for all sandstones sampled, with a slight enrichment in LREE over HREE (La_N/Yb_N = 1.12-1.64). Based on the observed REE trends the sandstones appear broadly similar with minor variation seen from samples 2009378006 and 2009378005 (Fig. 5). These results suggest a common or chemically similar provenance for all samples.

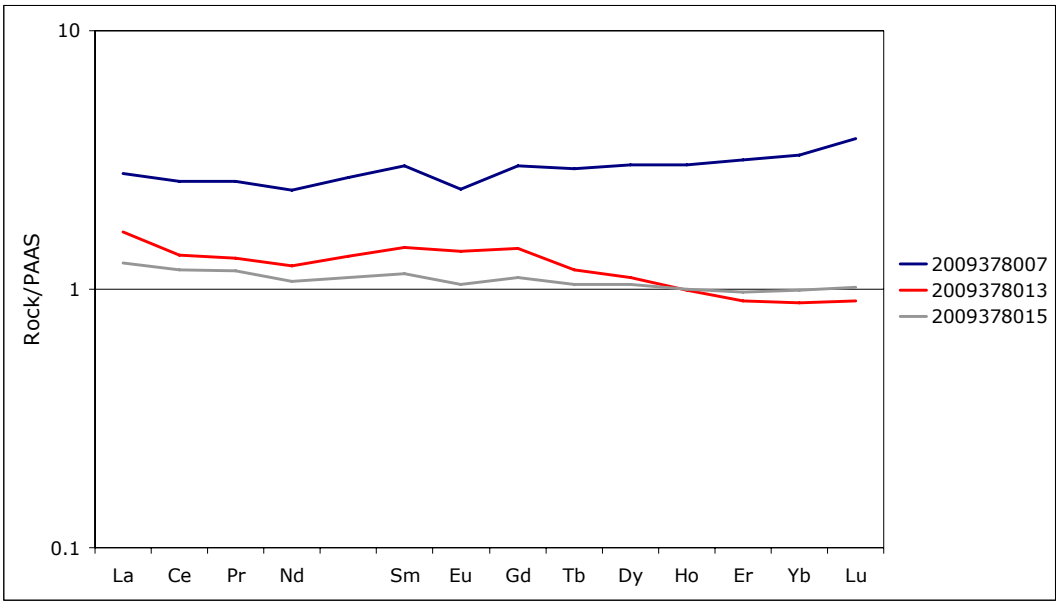

Figure 4: *Rare earth element data for mudstones from Bumbarlow 1. Values are normalised to PAAS of McLennan (1989).*

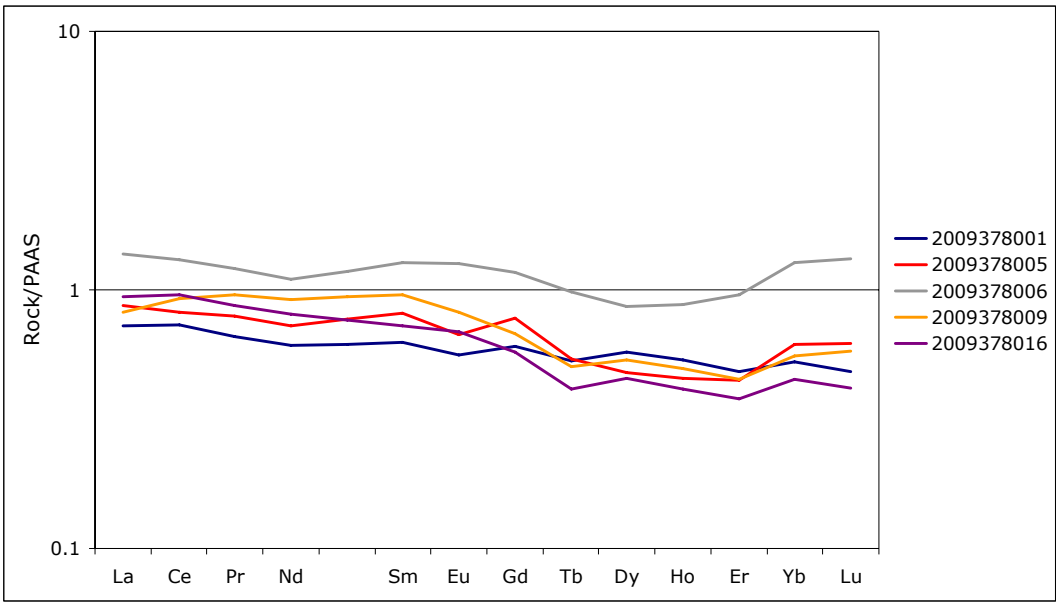

Figure 5: *Rare earth element data for sandstones from Bumbarlow 1. Values are normalised to PAAS of McLennan (1989).*

Mafic volcanics

Mafic volcanics were sampled from Bumbarlow 1 at depths of 546.2, 595.1, 635.0 and 655.0 m. Samples show significant alteration, with sample 2009378012 being the freshest. SiO_2 range 43.63 – 51.98 wt.%. Giles and Teale (1981), 58.02 wt.%. Harker variation diagrams show no systematic correlations between elements across the SiO_2 range. Rare earth element patterns are consistent for all samples (Fig. 6), indicating that the mafic magmas were derived from the same source region. The patterns reveal an enrichment in LREE over HREE (La_N/Yb_N = 4.9 - 6.8), and a marked Eu anomaly (Eu_N/Eu_N* = 0.71 - 0.51). Multi-element plots show a pronounced Nb-Ta anomaly, enrichment in incompatible elements, high Pb in some samples, and a negative Sr anomaly (Fig. 7).

Comparison with mafic volcanics in LNM10

One sample of mafic volcanics from LNM10 was analysed and compared with those in Bumbarlow 1. LNM10 was drilled 70 km to the south of Bumbarlow 1, and is situated approximately 10 km to the west of the 08GA-C1 seismic line. Mafic volcanics are intersected between 231.5 m and ~350 m, and volcaniclastic breccia between 350 m and 380 m (Fig. 8). The mafic volcanics are dark, with a 'peppery' amygdaloidal appearance. They are frequently brecciated, and often display jigsaw-fit textures. Between 295 m and 334 m, pillowed lava structures are observed suggesting subaqueous-aqueous lava emplacement. The breccia below ~350 m contains clasts of pink porphyritic volcanics similar to those intersected in Mudguard 1 (Curtis, 1990).

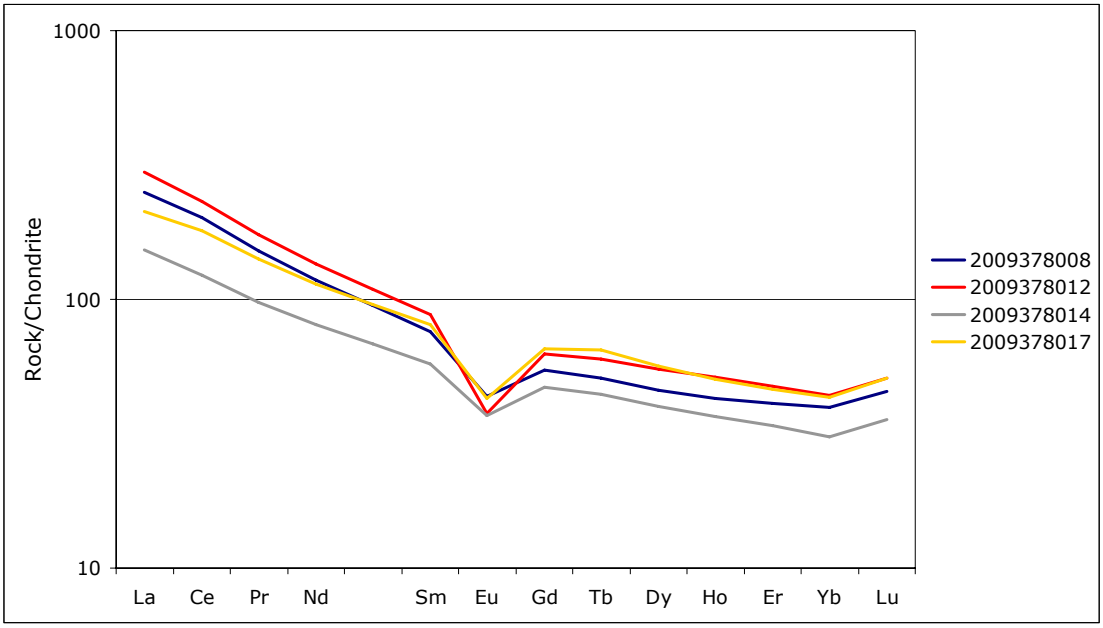

Figure 6: *Rare earth element data for mafic volcanics in Bumbarlow 1. Values are normalised to C1 chondrite of Sun and McDonough (1989).*

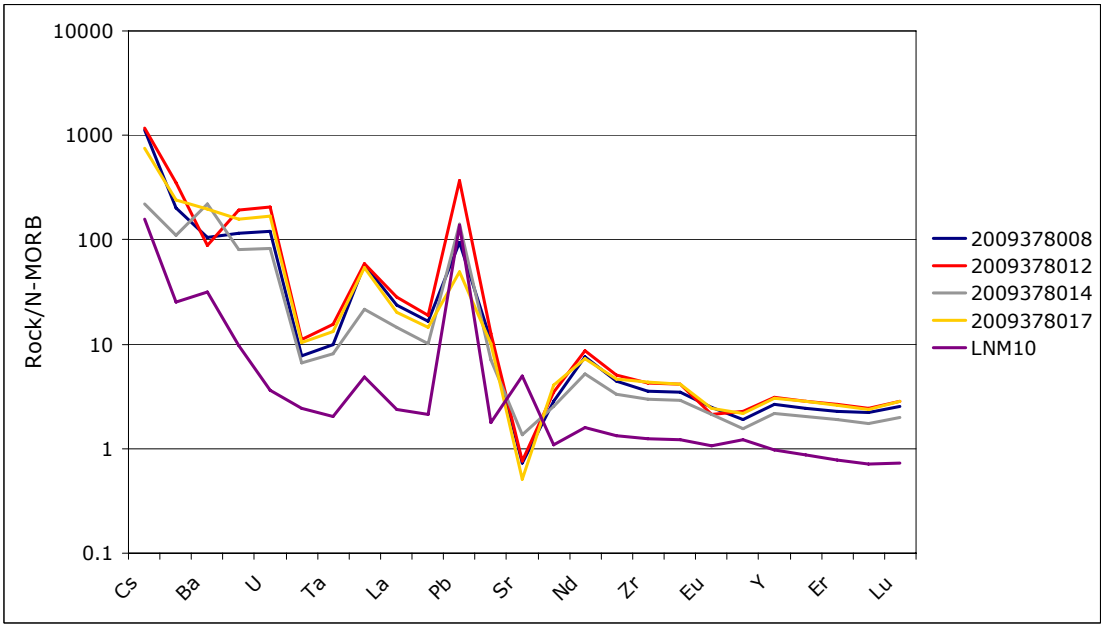

Figure 7: *Mafic volcanic samples analysed in this study normalised to N-MORB of Sun and McDonough (1989).*

The mafic volcanics in LNM10 have been attributed to the Benagerie Volcanics, which are equivalent to the voluminous Gawler Range Volcanics in the Gawler Craton to the east (eg., Fricke, 2008). Volcanics in Bumbarlow 1 have also been linked to mafic Gawler Range Volcanics (Giles and Teale, 1981). Mafic volcanics in LNM10 and Bumbarlow 1 show similar geochemical trends. Harker variation diagrams in Fricke (2008) indicate that the Bumbarlow 1 mafics form an evolutionary trend with volcanics in LNM10, although scatter in the data is high. On multi-element plots, volcanics from both holes show similar distributions, with enrichment in incompatible

elements and negative Nb anomalies. However, the degree of incompatible element enrichment is lower for LNM10 than for Bumbarlow 1, and LNM10 possesses a positive Sr anomaly (Fig. 7). Rare earth element patterns for LNM10 reveal a slight enrichment of LREE over HREE (La_N/Yb_N = 1.8 – 3.7) and Eu anomaly. These features are similar to the mafic volcanics in Bumbarlow 1, although REE abundances are markedly lower in LNM10. Overall, geochemical analyses suggest that mafic volcanics in LNM10 and Bumbarlow 1 are chemically similar and likely genetically related, with the Bumbarlow volcanics representing a more evolved member than those in LNM10.

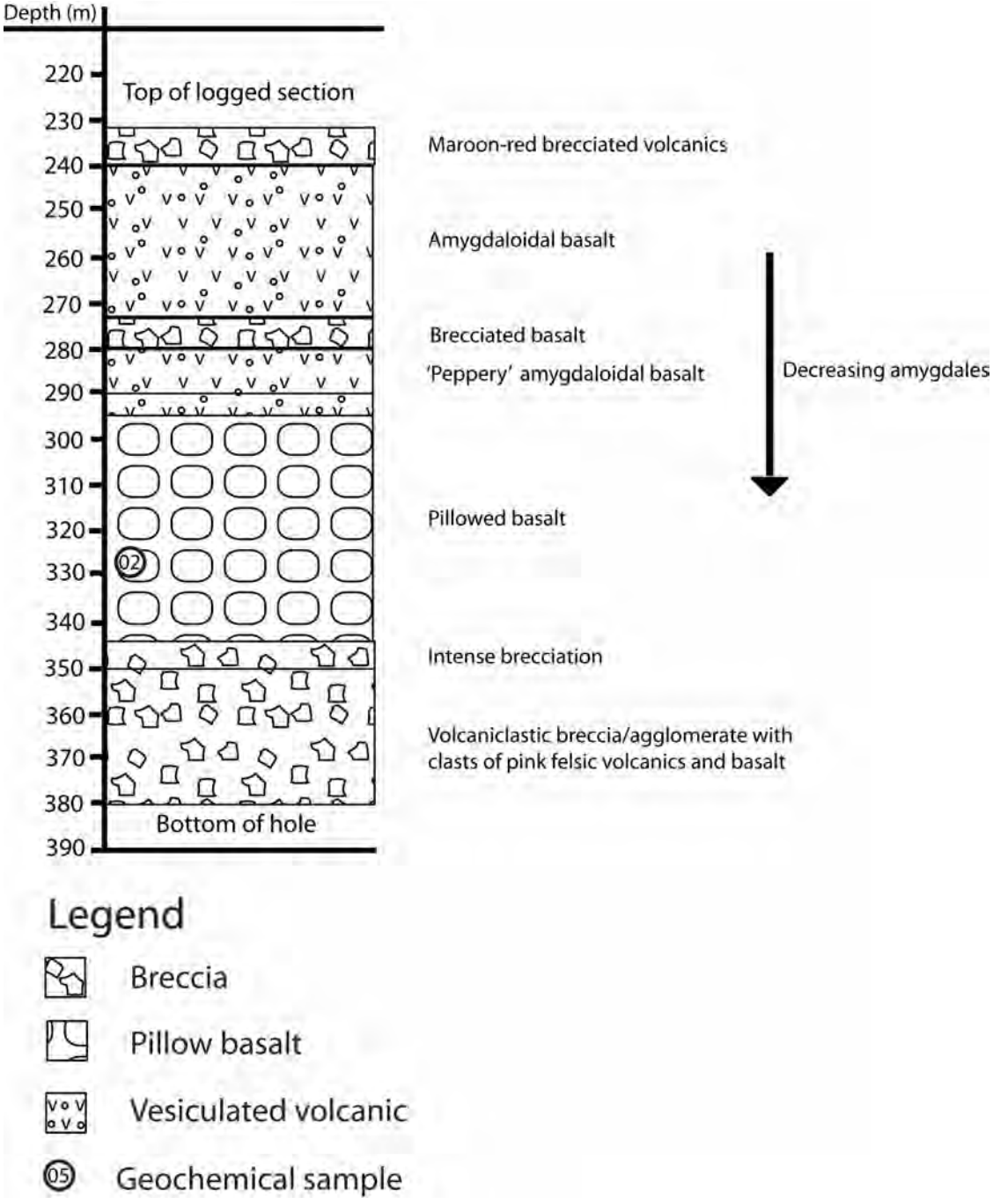

Figure 8 *Geological log of LNM10. The location of sample 2009378002 is also shown.*

GEOCHRONOLOGY

Previous geochronological work on Bumbarlow 1 yielded a whole rock Rb/Sr isochron age of 1360 ± 144 Ma from mudstone between 612.9 and 646.1 m (Youngs, 1978). Two samples were taken from Bumbarlow 1 to undertake SHRIMP detrital zircon geochronology. Details of the samples taken and analytical techniques are given by Fraser and Neumann (2010). Sandstone from the 'upper sediments package' (469.3- 474.6 m; sample 2009378006) gave a maximum depositional age of 1550 ± 6 Ma, while sandstone from the 'sediments and volcanics package' (686.0-691.0 m; sample 2009378001) yielded an older maximum depositional age of 1591 ± 6 Ma. Thus, the geochronology data suggests a shift in provenance between the deposition of the 'sediments and volcanics package' and the 'upper sediments package'. The 'upper sediments package' has also been suggested to be a lateral equivalent of the Pandurra Formation which has a whole rock Rb/Sr minimum deposition age of 1424 ± 51 Ma (Fanning et al., 1983). While this study cannot confirm this suggested Pandurra-Bumbarlow correlation, these new ages do not disprove the possibility of correlation either.

These data also help to constrain the age of the mafic volcanics in Bumbarlow 1. The sandstone sampled for geochronology in the 'sediments and volcanics package' underlies the mafic volcanics, and thus the volcanics must be younger than ~1591 Ma. Felsic volcanics intersected in the Culberta 1 and Mudguard 1 drill holes have been dated at 1585 ± 7 and 1585 ± 6 Ma respectively (Fricke, 2008). A further date of 1581 ± 4 Ma was also obtained from altered porphyritic rhyolite in Mudguard 1 by Fanning et al. (1998). Felsic volcanics have also been intersected in WK1. These volcanics form linear trends on Harker variation diagrams with the mafic volcanics in Bumbarlow 1 (Fricke, 2008). This suggests they may be the fractionation products of mafic rocks similar to those encountered in Bumbarlow 1 and LNM10 (Fig. 9). If this is correct, then the ~1585 Ma date for the felsic volcanics in Culberta 1 and Mudguard 1 may be tentatively interpreted as the magmatic age of the mafic volcanics in Bumbarlow 1. This is consistent with the age of the Gawler Range Volcanics in the Gawler Craton (Neumann and Fraser, 2007).

There are, however, complications with a ~1585 Ma age for the volcanics in Bumbarlow 1. For this age to be correct, then the sandstone interval immediately below the first volcanic horizon would have to have been deposited very close to its maximum depositional age of 1591 ± 6 Ma. Thus, this interpretation requires a mixed sedimentary-volcanic depositional system, which has not been definitively proven.

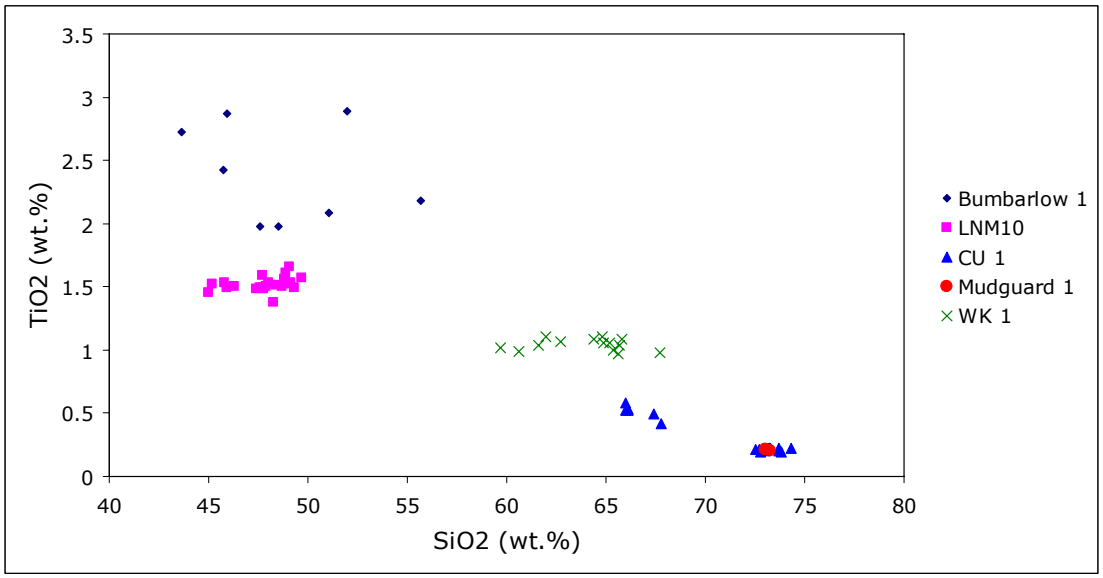

Figure 9: *Harker variation diagram showing mafic and felsic volcanics intersected in drill core in the Benagerie Ridge. Data for Bumbarlow 1 and LNM10 gathered in this study have been supplemented by data from CU1, Mudguard 1, and WK 1 from Fricke (2008).*

SPH1

SPH1 was drilled near the northern limit of the 08GA-C1 seismic transect and is situated ~10 km east of the line. It is located in the Moolawatana Domain of the Curnamona Province, which also includes the U-rich granites of the Mount Painter and Mount Babbage Inliers. The seismic package which SPH1 intersects is moderately reflective, and overthrusts the Neoproterozoic basin sediments (Korsch et al., 2010). Samples from SPH1 were taken to geochemically characterise and provide age constraints for this package.

Figure 10: *Typical banded calc-silicate from SPH1.*

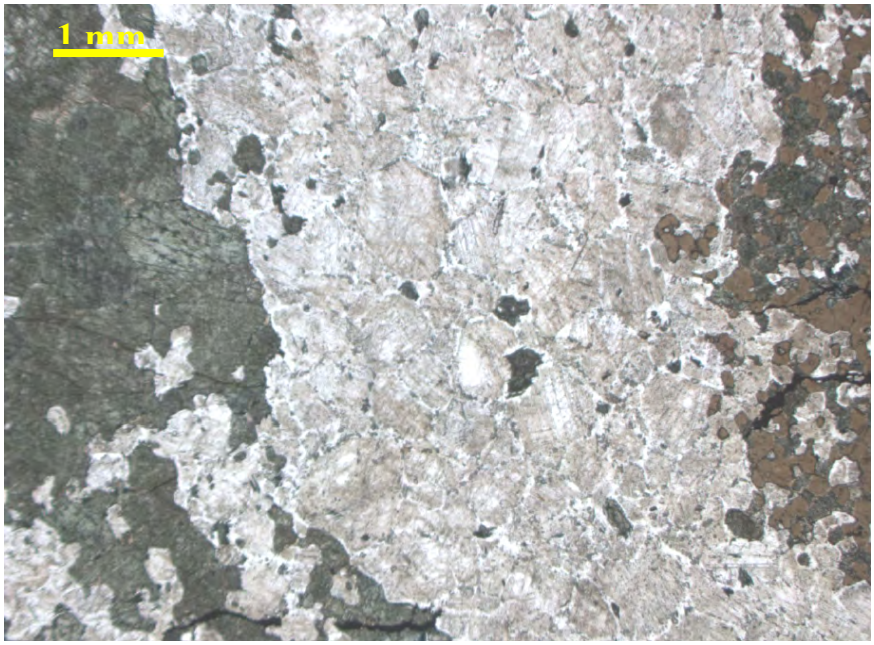

Figure 11: *Photomicrograph of sample 2009378037 from SPH1 taken at 1.6X magnification in transmitted light. The image shows chlorite, interlocking plagioclase and garnet crystals.*

GEOLOGICAL DESCRIPTION

Mesozoic and younger sediments are present to a depth of 413.5 m (Tahan and Dunbar, 1983). The Mesozoic sediments are underlain by an unnamed calc-silicate unit, which is present to the bottom of hole at 627 m (Fig. 10). It is crystalline, with variable textures throughout the length of the calc-silicate unit. It is generally banded or blotchy, with some sections having a gneissic appearance. Banded portions of SPH1 resemble the nearby Radium Creek Metamorphics (Sheard, 2009). Alteration is pervasive with variable colouration from bluish-grey to pistachio-green with quartzo-feldspathic zones appearing whiter.

Original logging (Tahan and Dunbar, 1983) describes the calc-silicate in SPH1 as hornfelsic gneiss; this is supported by thin section examination (Fig. 11). Sample 2009378027 was taken from 414.0-418.9 m for SHRIMP U-Pb zircon dating (Fig. 12). This sample is banded (even on the scale of the slide), and is typical of much of the calc-silicate. Bands are somewhat diffuse, and are defined by anhedral grains of epidote and plagioclase. Minor epidote also occurs in feldspar bands, and vice-versa. Crystals of both epidote and plagioclase have an interlocking texture, and share seriate boundaries with adjacent grains. Quartz is also present in lesser proportions to feldspar. Garnet is present in small amounts, and is associated with epidote. Minor calcite is observed in this sample, although it is more common in other samples as both veins and as individual crystals. Other samples also have chlorite as a major component, as well as pyroxene.

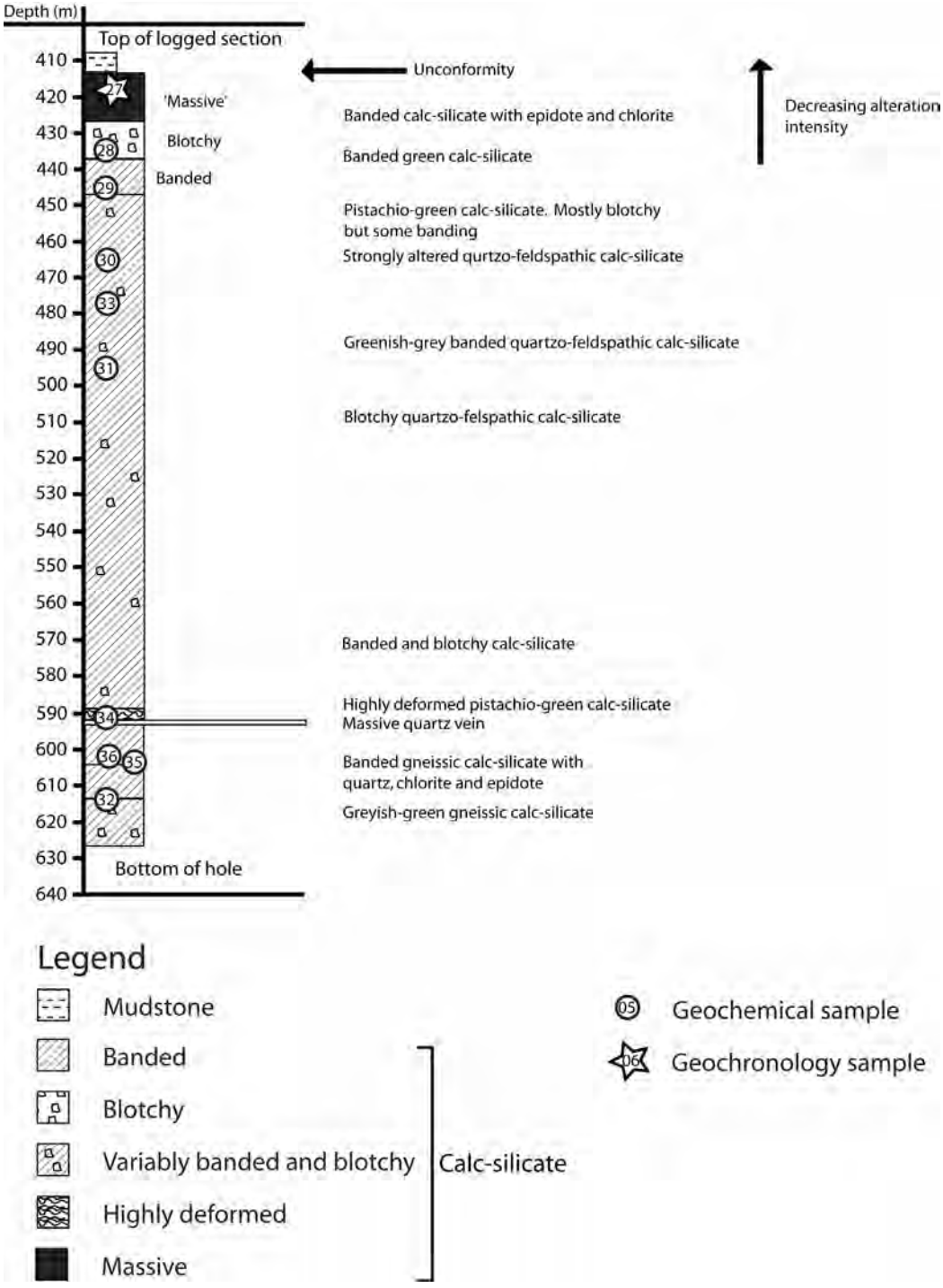

Figure 12: *Schematic geological log of SPH1. Sample locations are also shown.*

GEOCHEMISTRY

Ten samples were taken from SPH1 for geochemical analysis. These data are presented in Appendix 1. Due to the high degree of alteration in this sample, primary geochemical features may be completely obliterated. No systematic down-hole element variation has been detected, except perhaps for decreasing Zr and Hf with increasing drill hole depth. Other geochemical features include high Zn (typically >500 ppm, but up to 2072 ppm) and Fe (up to 14.9 wt.% total Fe_2O_3). Fe^{3+}/Fe^{2+} values are low (generally <0.74), indicating that these rocks are reduced. Rare earth element patterns are characterised by enriched LREE and flat MREE to HREE (Fig. 13). Most samples show a prominent Eu anomaly and exhibit a slight negative Tb anomaly, which may reflect partitioning of this element into garnet.

On both REE and multi-element plots, samples have the same general characteristics except 2009378034. This sample is characterised chemically by very low Rb, Ba and K, and almost absent Eu anomaly relative to other samples. The sample itself is highly altered and strongly deformed. Thin section examination reveals epidote as the dominant alteration mineral, with minor plagioclase present. This significant variation in mineralogy accounts for the observed variation in geochemistry.

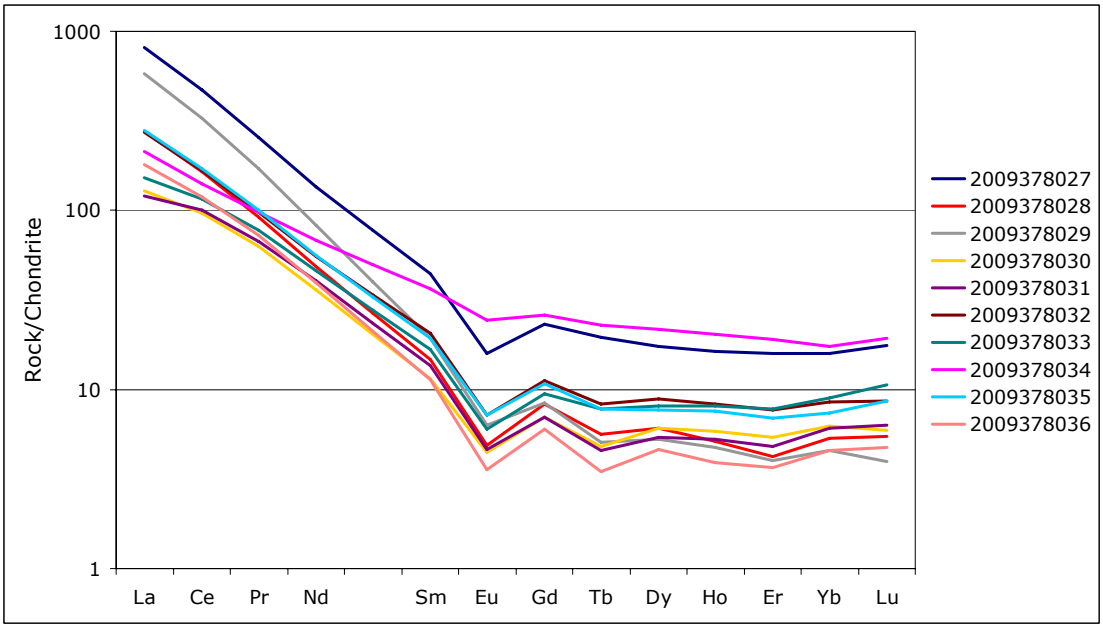

Figure 13: *Rare earth element data from SPH1. Values are normalised to C1 chondrite of Sun and McDonough (1989).*

GEOCHRONOLOGY

One sample from SPH1 was taken for SHRIMP U-Pb geochronology (2009378027). This sample was chosen because it was the least altered interval in the calc-silicate package. Details of the data and analytical techniques can be found in Fraser and Neumann (2010). Although there are two zircon populations (1585 ± 6 Ma (*n*=8) and 1558 ± 3 Ma (*n*=49)), an age of 1558 ± 3 Ma has been assigned for the calc-silicate protolith. This is interpreted to be a magmatic age since the zircon age spectrum is relatively confined and Th/U values of the analysed zircons are more typical of those expected for magmatic crystallisation. This would place the magmatic protolith of the SPH1 calc-

silicate as broadly coeval with U-rich intrusives in the Mount Painter and Mount Babbage Inliers (Neumann and Fraser, 2007).

BWM1A-1 and ETM5A-1

Drill holes BWM1A-1 and ETM5A-1 were drilled just south of the geophysically-defined extent of the Benagerie Volcanics (eg., Williams et al., 2009). BWM1A-1 is situated ~16 km south-southwest of LNM10 while ETM5A-1 was drilled ~21 km southeast of BWM1A-1 (Fig. 1). Both drill holes are west of the 08GA-C1 seismic line with BWM1A-1 12 km, and ETM5A-1 ~1 km from the line. Original core logs of BWM1A-1 record the presence of mottled and banded, pink to red volcanics (trachyte and rhyolite) from 391 m. Logs for ETM5A-1 record red to pink volcanics from 444 m similar to those described in BWM1A-1. Each drill hole was sampled to determine whether they represent extensions to the known distribution of the Benagerie Volcanics.

GEOLOGICAL DESCRIPTION

BWM1A-1

BWM1A-1 was examined from ~391 m to the bottom of hole at 600 m (Fig. 15). Below 391 m the rock is generally very fine-grained and strongly altered to a brick- to brownish-red colour (Fig. 14). It is often brecciated, and displays banded, mottled or massive textures. Banding is defined by layers of opaque-rich (magnetite) altered metasediment. Magnetite also occurs as disseminations and veins throughout the metasediment. Calcite is present in extensive veins and as cement in zones of intense brecciation (Fig. 14a). Fluorite was observed at ~542, 494 and 406 m, where it is associated with calcite and pyrite veining (Fig. 14b). Minor sulphides (chalcopyrite and pyrite) occur intermittently.

Although initially thought to be felsic volcanics, thin section inspection indicates that this section consists of strongly altered metasediments. The very fine grainsize in hand sample is due to extensive recrystallisation of original sedimentary grains, which have almost been destroyed. It is interpreted that this rock was probably originally a mudstone or very fine sand. The remnant banding observed may correspond to original sedimentary layering. The altered metasediments are unconformably overlain by Adelaidean clastic sediments. The base of the Adelaidean sequence is defined by a sharp contact between an angular conglomerate and the altered metasediment package. Clasts of the altered underlying package are present in the conglomerate, indicating that alteration occurred prior to the deposition of the Adelaidean sediments.

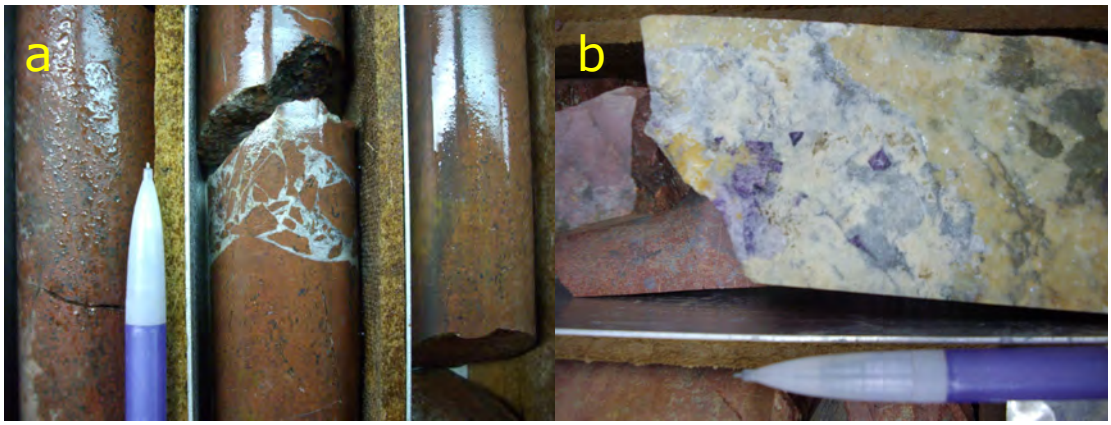

Figure 14: *Photographs of drill core from BWM1A-1 showing calcite infilling zones of intense brecciation (a), and fluorite (b).*

ETM5A-1

ETM5A-1 consists of Cenozoic to Adelaidean clastic and carbonate sedimentary rocks unconformably underlain by altered metasedimentary rocks from ~445 m to the bottom of hole at 541.5 m (Fig. 15). The metasediments in this hole have a very similar appearance to those in BWM1A-1. The core is characterised by a brownish- to brick-red appearance and very fine grainsize. It is commonly banded, and has a mottled appearance. Many sections of the core also have a distinct mottled appearance caused by small (<1-3 mm) brownish-white patches. It has been suggested that these represent pseudomorphs after scapolite within the original rock (R. Skirrow *pers. comm., 2010)*.

The original rock was probably similar to that in BWM1A-1 (ie., laminated mudstone or very fine sand), despite it being originally logged as sodic to potassic felsic volcanics (Moore, 1990). Banding observed in sample 2009378018 (444.80-449.2 m) probably reflects original sedimentary layering. Most of the rock has been strongly altered, which has destroyed many of the original textures. Alteration is dominated by K-feldspar, hematite, chlorite, calcite, magnetite and sericite. From examination of the limited number of thin sections available, it seems that the general paragenetic scheme is as follows: initial albitisation (R. Skirrow, *pers. comm., 2010*) is followed by alteration to a K-feldspar and magnetite assemblage. This is in turn overprinted by veins of magnetite and calcite, followed by chlorite. In one sample (2009378019; ~479 m), chlorite appears to pseudomorph amphibole, although this is not certain. Sericite alteration also occurs after the K-feldspar stage. Hematite alteration is ubiquitous, and may occur at any of the stages described above. This alteration assemblage is very similar to that observed in BWM1A-1, with the exception of the lack of sulphides and fluorite. This rock also appears to be less brecciated than BWM1A-1.

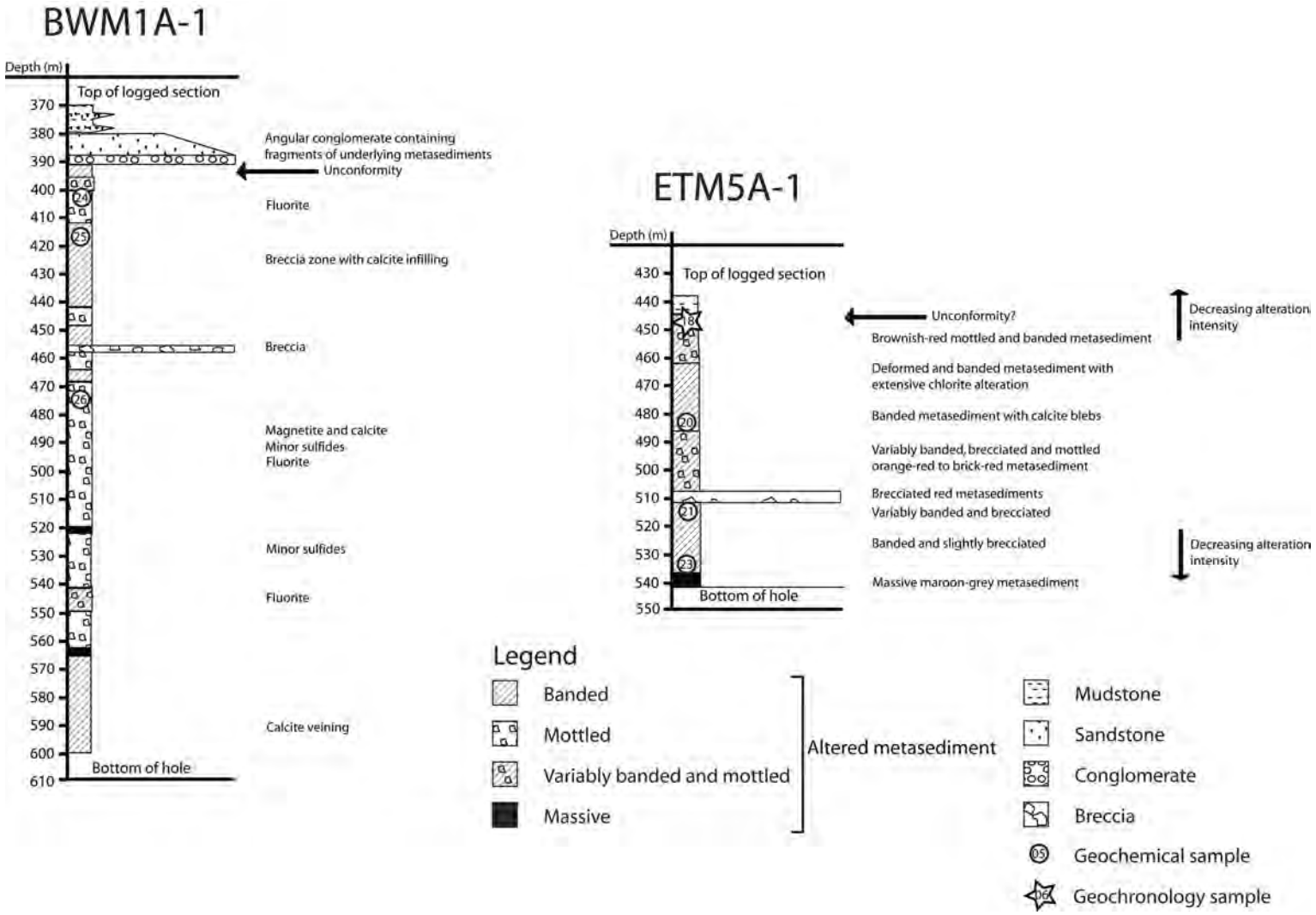

Figure 15: *Schematic logs for BWM1A-1 and ETM5A-1. Sample locations are also shown.*

GEOCHEMISTRY

Four samples from ETM5A-1 and three samples from BWM1A-1 were geochemically analysed. Rare earth element patterns for ETM5A-1 are essentially identical throughout the core. When normalised to chondritic abundances, LREE are enriched relative to HREE (La_N/Yb_N = 4.5-11.5), with a pronounced Eu anomaly. Abundances are close to those for PAAS (Fig. 16). On the other hand, REE patterns for BWM1A-1 are generally flat. Multi-element plots are also similar for both holes, except for high LREE and MREE in BWM1A-1.

The geochemistry of BWM1A-1 and ETM5A-1 is strongly disrupted by alteration. Although the alteration assemblages in these holes is reminiscent of those characteristic of IOCG systems (eg., Hitzman et al., 1992), elements typically associated with those systems (eg., Fe, Na, K, Cu, Au, LREE, F, Ba, P, U) are present in only moderate concentrations (Fig. 17). K_2O and Ba are high, F is moderate to high, and Na_2O is moderate. Total Fe content is not especially high, despite the pervasive hematite alteration observed. Fe^{3+}/Fe^{2+} for both ETM5A-1 and BWM1A-1 is high (1.49-6.55), indicating that these rocks are oxidised. These features suggest that the alteration in ETM5A-1 and BWM1A-1 may be a distal part of a broader IOCG alteration system (see also Burtt et al., 2004). In general, BWM1A-1 has a greater IOCG affinity than ETM5A-1.

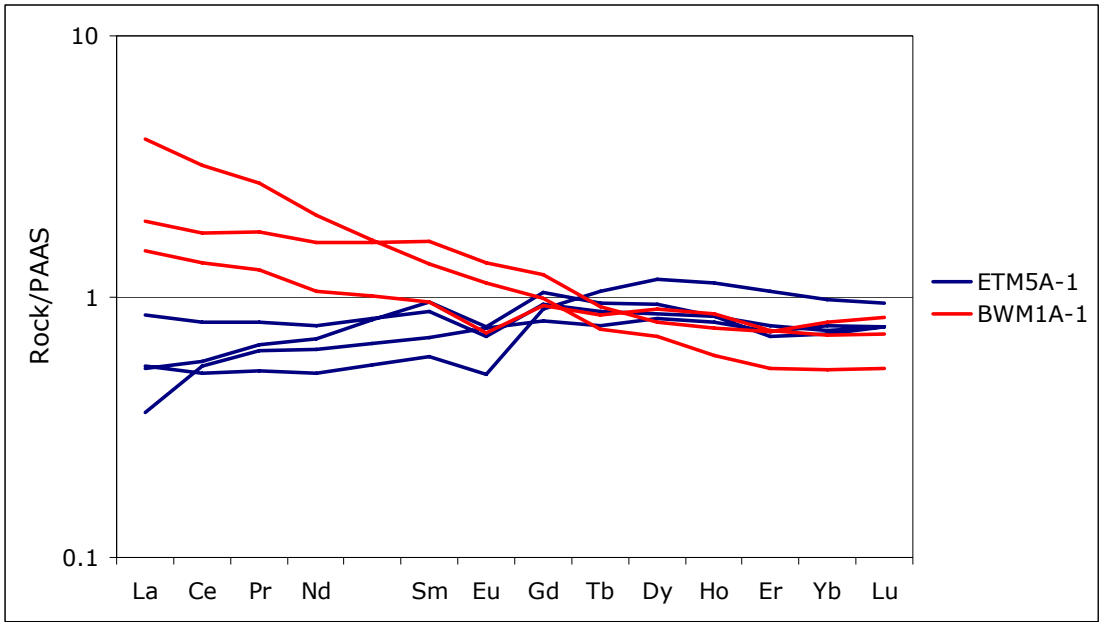

Figure 16: *Rare earth element data for ETM5A-1 and BWM1A-1. Values are normalised to PAAS of McLennan (1989).*

GEOCHRONOLOGY

One sample was taken from ETM5A-1 to constrain the age of the package. The sample was taken from 444.8 – 449.2 m (2009378018), and is reddish, banded, and altered. Although highly altered, and therefore not optimal for geochronology, it was not possible to avoid such alteration. After processing, the sample yielded ten zircons, of which four gave concordant ages (Fraser and Neumann, 2010). Three zircons combined to give an age of 1705 ± 5 Ma while the other grain yielded an age of 1623 ± 42 Ma. The low number of useful analyses render meaningful geochronological interpretation impossible (Fraser and Neumann, 2010).

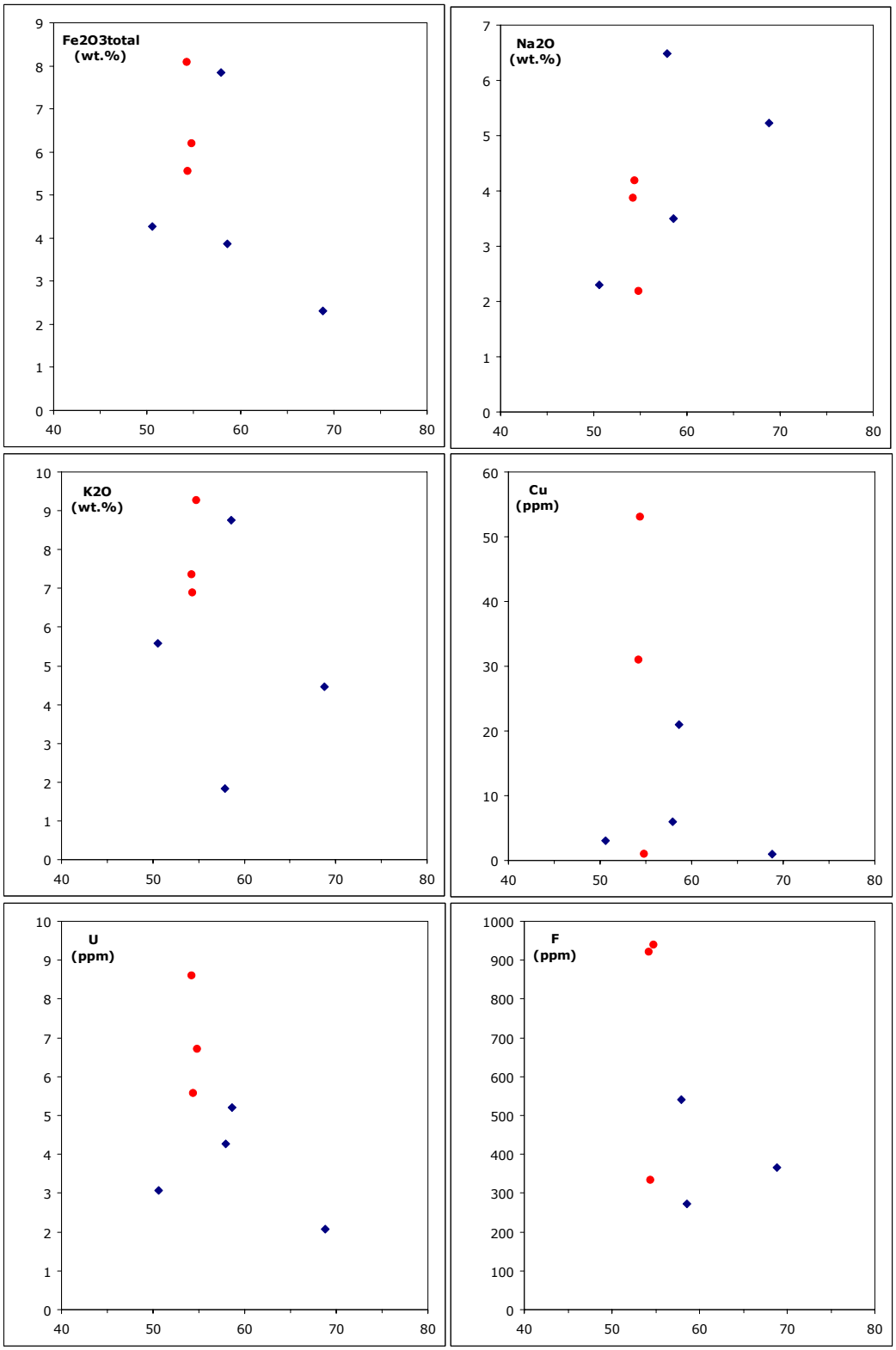

Figure 17: *Selected elements associated with IOCG mineralisation plotted against SiO_2 (wt.%) from BWM1A-1(red) and ETM5A-1 (blue).*

BRD012 and BRD013

Numerous granitic bodies mapped as Bimbowrie Suite in solid geology (Cowley, 2006) occur both underneath and proximal to the 08GA-C1 seismic line (red coloured units in Fig. 1). One such body occurs approximately 20 km east of CDP 9000. Two holes intersecting this unit (BRD012 and BRD013) were sampled to characterise the felsic intrusives in the vicinity of the seismic line. These holes were initially drilled to target potential IOCG mineralisation by Newcrest Mining Limited, and are situated approximately 500 m apart.

GEOLOGICAL DESCRIPTION

In hand sample, samples from both holes are strongly porphyritic. Pale coloured feldspar and quartz phenocrysts up to 9 mm are typically rounded (although some show lath-like morphologies) and are set in a finer grey groundmass. Mafic mineralogy is sparse. Light green phenocrysts are evident in hand sample, which probably represent altered mafic phases. Some sections of core are reddened by hematite alteration, which decreases down-hole.

In thin section (Fig. 18), the most striking feature is the strongly porphyritic nature of the rock. Phenocrysts of quartz and sericiticised K-feldspar are distributed evenly throughout the slide. Quartz forms large and often rounded phenocrysts, which frequently show embayed rims. K-feldspar also forms large crystals, which may be blocky, tabular, or more irregular forms. Some phenocrysts of feldspar display remnant albite twinning, indicating minor plagioclase. The phenocrysts are set in a very fine-grained groundmass of quartz and feldspar. These textural features indicate that the granite was intruded to high crustal levels. Mafic mineralogy is almost totally absent, and chlorite appears to have replaced remnant mafic mineralogy (probably biotite). Opaque minerals (?magnetite) are common, and occurs as secondary disseminations, or more rarely as veins cross-cutting phenocryst phases. Opaques are observed to replace chlorite, which suggests late emplacement in some cases. Accessory minerals are minor, and consist of zircon and fluorite, the latter of which appears to have a close spatial relationship to chlorite (or remnant mafic mineralogy).

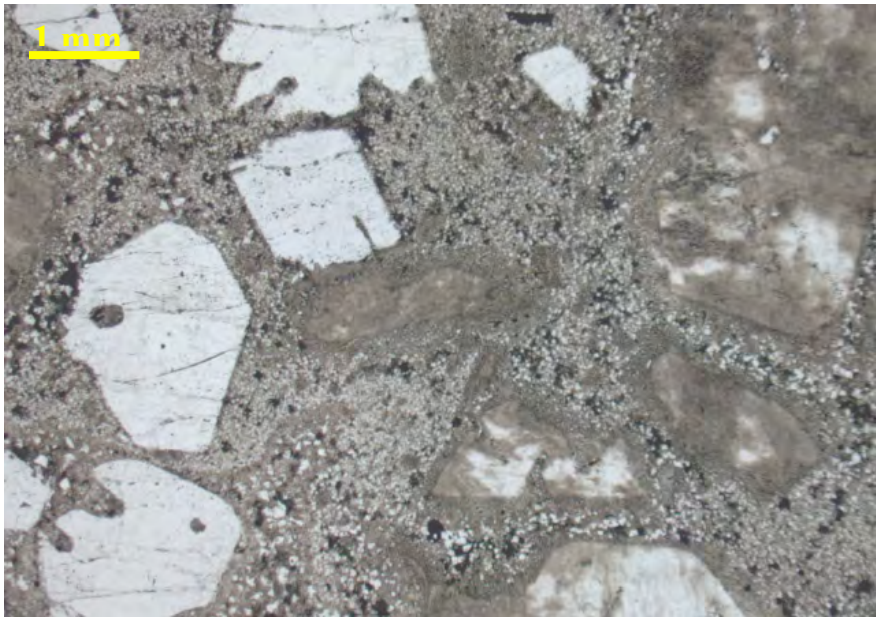

Figure 18: *Photomicrograph of sample 2009378038 taken at 1.6X magnification in transmitted light.*

GEOCHEMISTRY

Two samples from BRD012 (2009378038 and 2009378039) and one sample from BRD013 (2009378040) were geochemically analysed. The granite is fractionated, and samples from BRD012 are more evolved than those from BRD013, as indicated by SiO_2 content (68.9 wt.% compared with 73.2-73.4 wt.%) and Rb/Sr (5.9 compared with 16.2-19.7). All samples are very weakly peraluminous (ASI = 1.06-1.08), and probably evolved from an original mataluminous parental magma. Multi-element plots show enrichment in incompatible elements, and negative Ba, Nb-Ta, Sr, P and Ti anomalies (Fig. 19). Rare earth element patterns (Fig. 20) show overall high REE contents, enrichment of LREE over HREE (La_N/Yb_N = 7.7-7.9) and a pronounced Eu anomaly (Eu_N/Eu_N* = 0.41-0.19).

The granite intersected in BRD012 and BRD013 has several distinct geochemical features. All samples are characterised by high K_2O, total iron, HFSE (Nb, Y, Zr), Mo, REE, F, U, Ga, Pb, Zn and Ba. Tin is elevated, suggesting these granites are reduced. This is also suggested by relatively low Fe^{3+}/Fe^{2+} ratios (0.58-0.94). Zircon saturation temperatures (calculated according to Watson and Harrison, 1983) are moderately high (851-892°C). These geochemical features are reminiscent of A-type granites (Loiselle and Wones, 1979), and are comparable to values typical of A-type granites in the Lachlan Fold Belt (Whalen et al., 1987; King et al., 1997; Kemp and Hawkesworth, 2004). A-type discrimination diagrams from Whalen et al. (1987) confirm the A-type character of these magmas (Fig. 21). Using the granite classification schema of Frost et al. (2001), all samples are ferroan and peraluminous. Samples from BRD012 are alkali-calcic, while the sample from BRD013 is alkalic.

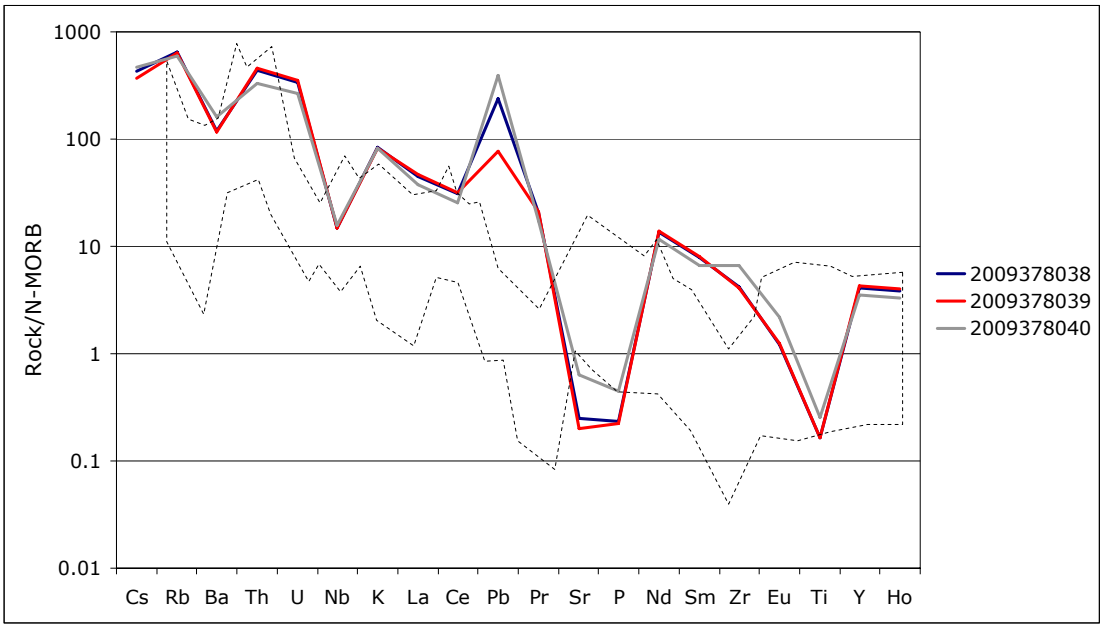

Figure 19: *Granite samples analysed in this study normalised to N-MORB of Sun and McDonough (1989). Bimbowrie Suite data range from Fricke (2008) is shown by the dashed line.*

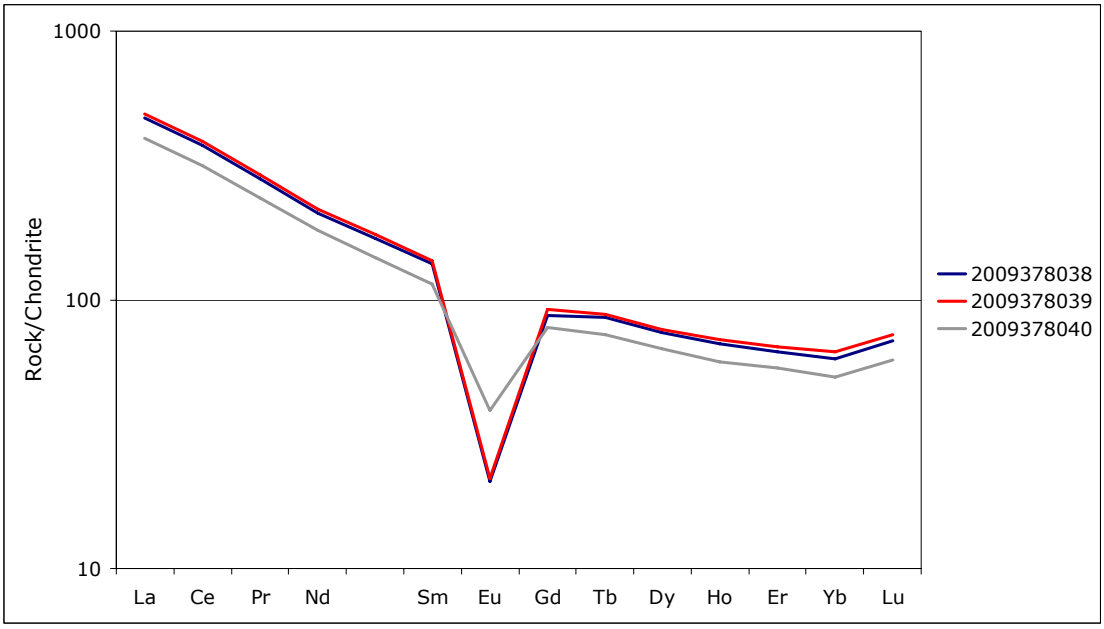

Figure 20: *Rare earth element patterns for granites from BRD012 and BRD013. Values are normalised to C1 chondrite of Sun and McDonough (1989).*

GEOCHRONOLOGY

SHRIMP U-Pb geochronology was undertaken on sample 2009378038 (BRD012, 482-488 m). This was the freshest rock sampled from BRD012 and BRD013. Analysis of the recovered zircons yields a magmatic crystallisation age of 1590 ± 5 Ma, with no inherited ages identified (Fraser and Neumann, 2010).

CORRELATIONS WITH OTHER GRANITIC UNITS

The age of the granite in BRD012 is synchronous with the extensive magmatism of the Bimbowrie Suite. The Bimbowrie Suite belongs to the Mesoproterozoic Ninnerie Supersuite, and consists of two-mica S-type granites interpreted to be derived from partial melting of Willyama Supergroup metasediments (Fricke, 2008). Multi-element plots reveal similar chemical features for the BRD012 and BRD013 samples and the Bimbowrie Suite (Fig. 19). However, the A-type character of the BRD012 and BRD013 granite is distinctly different to the S-type character of the Bimbowrie Suite. Thus, the granite described here does not correspond to the Bimbowrie Suite. Rather, they may be genetically related to ~1590 Ma brick-red granites with A-type affinities intersected at Emu Dam (Teale, 2000), or may be equivalents of the similarly aged Hiltaba Suite (Neumann and Fraser, 2007) in the Gawler Craton. Further geochemical (especially isotopic) work will be required to better understand these potential correlations.

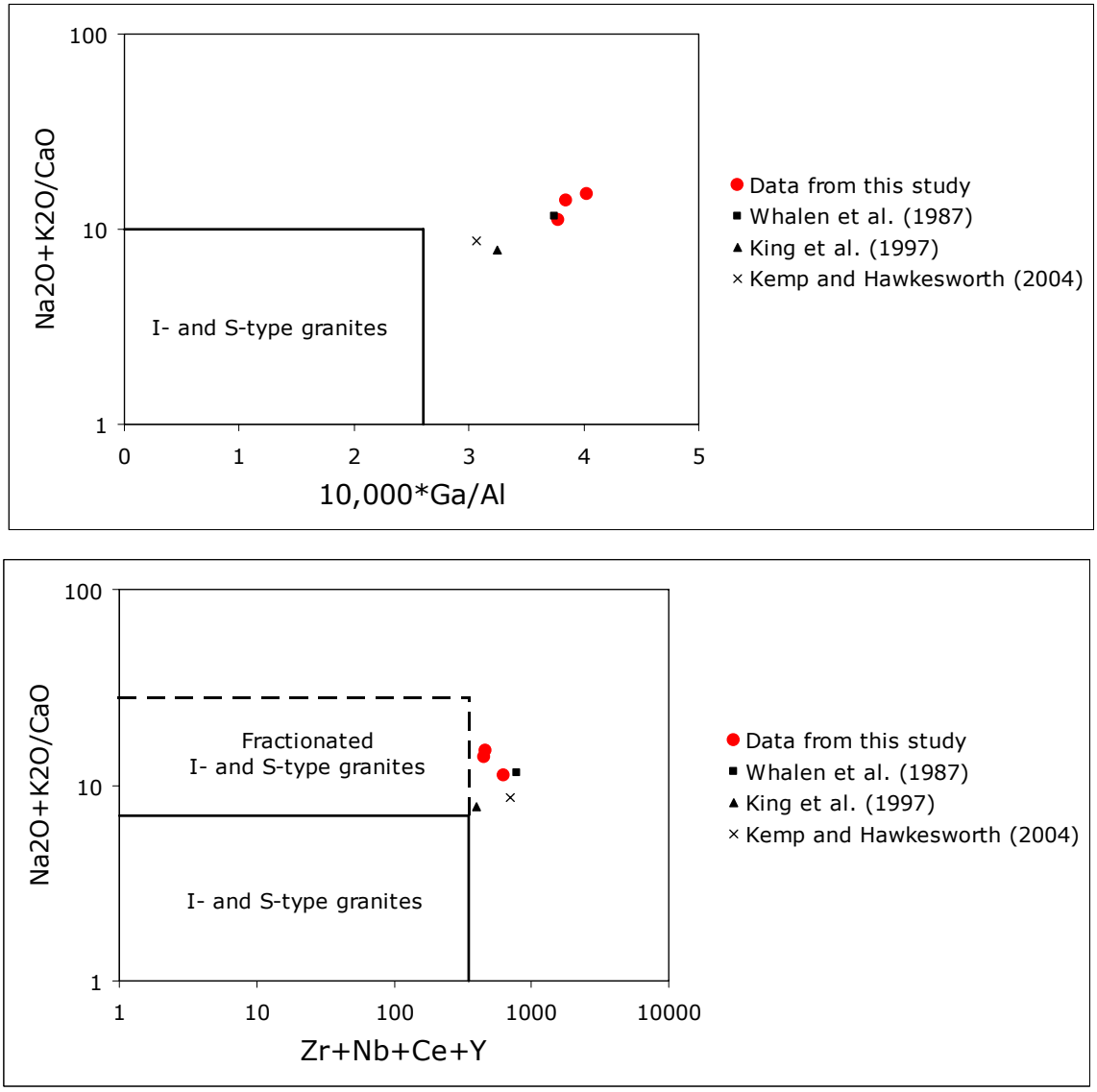

Figure 21: *Granite samples analysed in this study plotted on A-type discrimination diagrams from Whalen et al. (1987). Average A-type compositions from the Lachlan Fold Belt (Whalen et al., 1987; King et al., 1997; Kemp and Hawkesworth, 2004) have also been plotted for comparison.*

Summary and conclusions

The geochemical, geochronological and petrographic studies of this report and reassessment of pertinent previous work allows the following conclusions to be drawn:

- The stratigraphy intersected in Bumbarlow 1 may be divided into four main packages, as shown in Figure 2. The unconformity with the 'basal shale' at ~702 m separates this package (?Willyama Supergroup) from the overlying 'sediments and volcanics package'. Clasts of mafic volcanics from the 'sediments and volcanics package' in the conglomerate at the base of the 'upper sediments package' suggest the presence of an unconformity separating the 'sediments and volcanics package' from the 'upper sediments package' at ~509 m. This is itself overlain by Cenozoic to Mesozoic sediments.

- The geochronology and geochemistry indicate at least one shift in provenance during the deposition of the stratigraphy intersected in Bumbarlow 1. Ages obtained suggest that provenance shifted from material contemporary with the ~1590 Ma Bimbowrie Suite or ~1585 Ma granites from Mount Painter in the sandstone immediately underlying the mafic volcanics, to ~1550 Ma material. This younger material is potentially derived from granites equivalent to those in the Mount Painter Inlier. The previously obtained whole rock Rb/Sr age of 1360 ± 144 Ma (Youngs, 1978) is consistent with this data. These dates also allow (but do not confirm) correlation with the 1424 ± 51 Ma (Fanning et al., 1983) Pandurra Formation, as suggested by Teale and Flint (1995).

- The mafic volcanics in Bumbarlow 1 bear many geochemical similarities to those intersected in LNM10. However, Bumbarlow 1 volcanics are slightly more evolved. These two volcanic units are therefore interpreted to be genetically related. The age of the Bumbarlow 1 volcanics is still subject to uncertainty, but it is likely they were emplaced between ~1590 and ~1550 Ma. If they represent parental magmas to felsic volcanics intersected elsewhere in the Benagerie Ridge, then a date of around 1585 Ma may be assigned.

- The calc-silicate package intersected in SPH1 represents a hornfelsic gneiss unit with an igneous protolith of similar magmatic age to that obtained from granites in the Mount Painter Inlier. These potentially correspond to calc-silicates found within the Radium Creek Metamorphics (Sheard, 2009), although geochronological evidence is conflicting. These rocks have anomalous Zn.

- The fine-grained, pink-red lithology intersected in drill holes BWM1A-1 and ETM5A-1 is not volcanic, as previous logging has recorded. Despite the pervasive alteration in both holes, it is likely that the original lithology was mudstone or very fine sandstone. Hence, they do not extend the known extent of the Benagerie Volcanics. Alteration occurred prior to the deposition of the overlying Adelaidean sediments, as these incorporate clasts of the altered underlying lithology, while they themselves are not altered. Alteration in these holes is reminiscent of that in IOCG mineral systems, and suggests strong potential for IOCG mineralisation in the Curnamona Province.

- The identification of a ~1590 Ma A-type granite in the Benagerie Ridge is significant. These are potentially correlatives of the voluminous Hiltaba Suite granitoids in the Gawler Craton, which are of the same general age (Neumann and Fraser, 2007). These granites are also broadly contemporary with A-type felsic rocks of the Benagerie Volcanics which have been intersected in

drill core, and are considered to be equivalents of the Gawler Range Volcanics (Fricke, 2008). Thus, there is a potential association between granites sampled this study and the Benagerie Volcanics. This may be compared with the Hiltaba Suite-Gawler Range Volcanics association in the Gawler Craton. Considered together with the IOCG-like alteration styles observed in BWM1A-1 and ETM5A-1, the presence of A-type magmas reaffirms that this region has high potential for IOCG mineralisation (Teale, 2000; Burtt et al., 2004).

Acknowledgements

Bridgette Lewis and Simon van der Wielen are thanked for their helpful reviews of this record. Geochronological analysis was performed by Narelle Neumann. Bill Pappas and Liz Webber are recognised for rapidly processing and analysing the geochemical samples. Appreciation goes to Colin Conor and Claire Fricke (PIRSA) for assisting with viewing the drill holes and for sharing their knowledge of South Australian geology. The staff at the PIRSA core facility in Adelaide are greatly thanked for assisting with core viewing and sampling.

References

Burtt, A., Conor, C. and Robertson, S., 2004. Curnamona - an emerging Cu-Au province. MESA Journal, 33, 9-17pp.

Conor, C. H. H. and Preiss, W. V., 2008. Understanding the 1720-1640 Ma Palaeoproterozoic Willyama Supergroup, Curnamona Province, southeastern Australia: implications for tectonics, basin evolution and ore genesis. Precambrian Research, 166, 297-317pp.

Cowley, W. M., 2006. Solid geology of South Australia: peeling away the cover. MESA Journal, 43, 4-15pp.

Curtis, J. L., 1990. Anomaly M10. Drill hole LNM10-1. Appendix 3/7.2. Geological log. In: EL 522, EL 911 and EL 1203, Emu Dam. Progress reports for the period 27/8/79 to 13/3/88. South Australia Department of Mines, Open File Envelope No. 3614 (unpublished), 203-228pp.

Fanning, C. M., Ashley, P. M., Cooke, N. D. J., Teale, G. S. and Conor, C. C. H., 1998. A geochronological perspective of crustal evolution in the Curnamona Province. Geoscience Australia Record 1998/25. G. M. Gibson (ed). 30-35pp.

Fanning, C. M., Flint, R. B. and Preiss, W. V., 1983. Geochronology of the Pandurra Formation. Geological Survey of South Australia Quarterly Geological Notes, 88, 11-16pp.

Fleet, A. J., 1984. Aqueous and sedimentary geochemistry of the rare earth elements. P. Henderson (ed). Rare earth element geochemistry. Elsevier. 343-373pp.

Fraser, G. L. and Neumann, N. L., 2010. New SHRIMP U-Pb zircon ages from the Gawler Craton and Curnamona Province, South Australia, 2008-2010. Geoscience Australia Record 2010/16.

Fricke, C. E., 2008. Definitions of Mesoproterozoic igneous rocks of the Curnamona Province: the Ninnerie Supersuite. PIRSA Report Book 2008/4.

Frost, B. R., Barnes, C. G., Collins, W. J., Arculus, R. J., Ellis, D. J. and Frost, C. D., 2001. A geochemical classification for granitic rocks. Journal of Petrology, 41, 2033-2048pp.

Gibson, G., Drummond, B., Fomin, T., Owen, A., Maidment, D., Gibson, D., Peljo, M. and Wake-Dyster, K., 1998. Re-evaluation of crustal structure of the Broken Hill Inlier through structural mapping and seismic profiling. Australian Geological Survey Organisation Record 1998/11.

Giles, C. W. and Teale, G. S., 1981. An investigation of altered volcanic rocks in Bumbarlow 1. South Australia Geological Survey Quarterly Geology Notes, 71, 13-18pp.

Goleby, B. R., Korsch, R. J., Fomin, T., Conor, C. H. H., Preiss, W. V., Robertson, R. S. and Burtt, A. C., 2006. The 2003-2004 Curnamona Province seismic survey. Geoscience Australia Record 2006/12.

Hitzman, M. W., Oreskes, N. and Einaudi, M. T., 1992. Geological characteristics and tectonic setting or Proterozoic iron oxide (Cu-U-Au-REE) deposits. Precambrian Research, 58, 241-287pp.

Jenner, G. A., Longerich, H. P., Jackson, S. E. and Fryer, B. J., 1990. ICP-MS - a powerful tool for high-precision trace-element analysis in earth sciences: evidence from analysis of selected USGS reference samples. Chemical Geology, 83, 133-148pp.

Kemp, A. I. S. and Hawkesworth, C. J., 2004. Granitic perspectives on the generation and secular evolution of the continental crust. Treatise on Geochemistry. H. D. Holland and K. K. Turekian (ed). Amsterdam, Elsevier. 3, 349-410pp.

King, P. L., White, A. J. R., Chappell, B. W. and Allen, C. M., 1997. Characterization and origin of aluminous A-type granites from the Lachlan Fold Belt, southeastern Australia. Journal of Petrology, 38, 371-391pp.

Korsch, R. J., Preiss, W. V., Blewett, R. S., Fabris, A. J., Neumann, N. L., Fricke, C. E., Fraser, G. L., Holzschuh, J., Milligan, P. R. and Jones, L. E. A., 2010. Geological interpretation of deep seismic reflection and magnetotelluric line 08GA-C1: Curnamona Province, South Australia.

In: R. J. Korsch and N. Kositcin (eds). South Australian seismic and MT workshop 2010. Geoscience Australia Record 2010/10, 42-53pp.

Loiselle, M. C. and Wones, D. R., 1979. Characteristics and origin of anorogenic granites. Geological Society of America Abstracts with Programs, 11, 468pp.

McLennan, S. M., 1989. Rare earth elements in sedimentary rocks: influence of provenance and sedimentary processes. Geochemistry and mineralogy of rare earth elements. In: B. R. Lipin and G. A. McKay (eds). Reviews in Mineralogy. 21, 169-200pp.

Moore, M., 1990. Anomaly M5. Appendix 1/5.3. Geological Log. In: EL 522, EL 911 and EL 1203, Emu Dam. Progress reports for the period 27/8/79 to 13/3/88. South Australia Department of Mines and Energy Open File Envelope 3614 (unpublished), 114-139pp.

Neumann, N., Sandiford, M. and Foden, J., 2000. Regional geochemistry and continental heat flow: implications for the origin of the South Australian heat flow anomaly. Earth and Planetary Science Letters, 183, 107-120pp.

Neumann, N. L. and Fraser, G. L., 2007. Geochronological synthesis and time-space plots for Proterozoic Australia. Geoscience Australia Record 2007/06.

Norrish, K. and Chappell, B. W., 1977. X-ray fluorescence spectrometry. Physical methods in determinative mineralogy, 201–272pp.

Pyke, J., 2000. Minerals laboratory staff develops new ICP-MS preparation method. AGSO-Geoscience Australia Research Newsletter, 33, 12-14pp.

Robertson, R. S., Preiss, W. V., Crooks, A. F., Hill, P. W. and Sheard, M. J., 1998. Review of the Proterozoic geology and mineral potential of the Curnamona Province in South Australia. PIRSA Report Book 98/3.

Rollinson, H., 1993. Using geochemical data: evaluation, presentation, interpretation. Harlow, Longman Group UK Ltd.

Sheard, M. J., 2009. Explanatory notes for CALLABONNA 1:250 000 geological map, sheet SH 54-6. PIRSA Report Book 2009/1.

Skirrow, R. G., 2009. Uranium ore-forming systems of the Lake Frome region, South Australia: regional spatial controls and exploration criteria. Geoscience Australia Record 2009/40.

Skirrow, R. G. and Ashley, P. M., 2000. Proterozoic Cu-Au systems of the Curnamona Province-members of a global family? MESA Journal, 19, 48-50pp.

Sun, S. S. and McDonough, W. F., 1989. Chemical and isotope systematics of oceanic basalts: implications for mantle composition and processes. Magmatism in the Ocean Basins. A. D. Saunders and M. J. Norry (ed). Geological Society of London Special Paper 42. 313-345pp.

Tahan, G. and Dunbar, G. J., 1983. EI 567, 963 (EX EL 209) Paralana, SA progress report from 18/3/80 to Feb. 1983, for BP Minerals. South Australia Department of Mines and Energy Open File Envelope 3745.

Teale, G. S., 2000. Known and potential mineralisation styles, Benagerie Ridge Magnetic Complex. MESA Journal, 19, 43-45pp.

Teale, G. S. and Flint, R. B., 1995. Curnamona Craton and Mount Painter Province. In: J. F. Drexel, W. V. Preiss and A. J. Parker (eds).The Geology of South Australia. Volume 1: The Precambrian. 147-148pp.

Watson, E. B. and Harrison, T. M., 1983. Zircon saturation revisited: temperature and composition effects in a variety of crustal magma types. Earth and Planetary Science Letters, 64, 295-304pp.

Whalen, J. B., Currie, K. L. and Chappell, B. W., 1987. A-type granites: geochemical characteristics, discrimination and petrogenesis. Contributions to Mineralogy and Petrology, 95, 407-419pp.

Williams, H. A., Betts, P. G. and Ailleres, L., 2009. Constrained 3D modelling of the Mesoproterozoic Benagerie Volcanics, Australia. Physics of the Earth and Planetary Interiors, 173, 233-253pp.

Wilson, T. and Fairclough, M., 2009. Uranium and uranium mineral systems in South Australia. PIRSA Report Book 2009/14.

Youngs, B. C., 1978. Bumbarlow 1 - well completion report. PIRSA Report Book 78/117.

Appendix 1: Geochemical data

sample no	2009378001	2009378002	2009378005	2009378006	2009378007	2009378008	2009378009	2009378012	2009378013	2009378014	2009378015	2009378016	2009378017	2009378018
hole	Bumbarlow 1	LNM 10 1	Bumbarlow 1	Bumbarlow 1	Bumbarlow 1	Bumbarlow 1	Bumbarlow 1	Bumbarlow 1	Bumbarlow 1	Bumbarlow 1	Bumbarlow 1	Bumbarlow 1	Bumbarlow 1	ETM5A 1
lithology	Sandstone	Mafic volcanic	Sandstone	Sandstone	Mudstone	Mafic volcanic	Sandstone	Mafic volcanic	Mudstone	Mafic volcanic	Mudstone	Sandstone	Mafic volcanic	Altered metasediment
Depth from	686.0	329.5	449.0	469.3	491.3	546.2	549.0	595.1	607.4	635.5	642.0	652.0	655.0	444.8
Depth to	691.0	330.0	450.0	474.6	491.8	546.7	553.6	595.6	607.9	636.0	642.5	653.0	655.5	449.2
SiO2	85.79	49.15	84.27	78.94	58.20	45.74	81.08	51.98	73.66	48.55	64.13	82.99	43.63	57.91
TiO2	0.20	1.53	0.32	0.52	1.09	2.42	0.26	2.89	0.35	1.98	0.61	0.19	2.73	0.55
Al2O3	5.98	13.64	5.12	7.34	19.58	13.34	6.69	12.73	11.32	13.77	16.28	6.92	13.04	14.15
FeO	1.23	8.90	0.36	0.49	1.06	10.06	1.32	8.66	2.50	7.43	4.83	1.84	1.81	3.02
Fe2O3	0.56	2.30	6.13	6.89	7.83	5.79	3.53	3.31	1.80	4.65	2.05	1.26	13.11	4.49
MnO	0.12	0.38	0.01	0.02	0.09	0.29	0.02	0.13	0.07	0.22	0.06	0.03	0.27	0.15
MgO	0.44	6.32	0.11	0.16	0.59	5.30	0.26	4.55	1.38	5.16	1.62	0.42	2.18	1.01
CaO	0.50	7.70	0.06	0.05	0.10	2.14	0.26	2.09	0.44	3.46	0.36	0.24	7.70	3.27
Na2O	0.03	4.77	<0.01	<0.01	0.14	0.17	0.09	0.80	0.11	4.20	0.16	0.08	0.77	6.49
K2O	2.24	0.35	1.55	2.22	5.91	4.18	4.37	4.26	5.03	1.57	4.74	2.95	3.90	1.83
P2O5	0.06	0.13	0.06	0.06	0.10	0.33	0.06	0.41	0.26	0.30	0.15	0.03	0.47	0.14
SO3	0.03	0.03	0.01	0.02	0.01	0.01	0.02	0.06	0.01	0.27	0.05	0.01	0.19	0.07
F	532	256	866	988	1391	926	883	1478	965	985	1286	809	681	541
Be	2.1	1.1	1.7	2.8	10.9	7.8	1.8	5.9	3.3	2.5	3.7	1.7	4.1	2.1
Sc	2.8	50	4.8	7.3	19.1	47.5	4.2	43	10.1	45.7	13.1	4	42.8	11.9
V	17	332	37	52	58	374	32	303	64	365	77	26	375	74
Cr	12	246	23	18	33	8	15	12	40	44	79	13	11	59
Ni	4	129	6	12	25	9	1	<1	23	<1	28	5	<1	14
Cu	20	177	4	5	19	7	6	91	37	10	34	3	5	6
Zn	25	473	23	43	207	502	11	786	124	189	142	50	388	21
Ga	6.1	18.8	7.2	10.6	33.5	27.2	8.1	25.8	17.5	23.7	23.1	7.8	24.8	20.1
Ge	0.9	1.4	1.6	1.6	2.8	2.1	1.2	1.9	1.4	1.6	2	1.4	1.8	1.1
As	7.5	77	16.1	24.9	150	68.4	23.7	106.4	6.4	45.6	10.8	10	49.8	8.2
Rb	101.5	14.3	93.4	104.9	319.1	113.3	169	197.4	223.7	62.3	313.2	128.8	135.7	84.3
Sr	27.4	443.3	135.8	160.7	288	65.2	50.9	69.1	41.8	123.6	44.5	40.6	46.3	50.9
Y	15.6	27.3	13.5	24.7	87.1	74.3	14.3	87.3	30.4	60.3	30.5	12.6	85.3	22.9
Zr	122.4	91.2	168.3	266.5	474.4	262.2	177	312.2	128.1	221.5	175.4	165.2	319.9	154.4
Nb	7.3	5.6	11.1	18.2	40.3	17.9	9.3	25.8	10.1	15.3	17.2	7.1	23.9	13.7
Mo	0.8	0.4	3	1.8	1.4	1.1	1.5	9.5	<0.3	0.9	<0.3	0.6	1.6	<0.3
Ag	<0.6	<0.6	<0.6	<0.6	<0.6	<0.6	<0.6	<0.6	<0.6	<0.6	<0.6	<0.6	<0.6	<0.6
Cd	<0.02	0.84	<0.02	<0.02	<0.02	<0.02	<0.02	0.12	<0.02	0.16	<0.02	<0.02	<0.02	<0.02
Sn	1	0.7	1.6	2.3	6.2	3.4	1.3	4.7	2.1	1.9	3.1	1	3.8	2.8
Sb	<0.8	<0.8	1.1	2.7	6.9	1.7	<0.8	3.2	<0.8	<0.8	0.8	<0.8	2.3	1.6
Cs	5.09	1.1	1.84	2.48	25.06	7.92	3.64	8.29	8.41	1.53	28.35	5.71	5.21	2.32
Ba	187.5	197.4	61.1	92.2	421.1	659.8	960.7	559.2	511.4	1383	531.6	538.7	1240	209.3
La	27.85	5.98	33.15	52.47	107	59.14	31.23	70.59	63.84	36.19	48.46	36.01	50.15	13.7
Ce	58.51	16.11	65.07	104.4	208	123.3	73.53	142	107.9	75.61	94.55	76.3	109.8	43.29
Pr	5.81	2.36	6.96	10.72	23.08	14.34	8.43	16.56	11.69	9.29	10.39	7.72	13.42	5.45
Nd	20.68	11.53	24.55	37.27	82.1	54.93	31.08	63	41.71	37.61	36.19	27.35	53.29	21.15
Sm	3.48	3.51	4.52	7.05	16.65	11.63	5.33	13.46	8.08	8.8	6.39	4.02	12.33	3.85
Eu	0.606	1.085	0.725	1.366	2.643	2.525	0.884	2.187	1.513	2.152	1.131	0.747	2.489	0.815
Gd	2.82	4.14	3.61	5.45	14.04	11.18	3.17	12.9	6.72	9.65	5.16	2.67	13.44	3.77
Tb	0.41	0.72	0.42	0.76	2.26	1.9	0.39	2.24	0.92	1.66	0.81	0.32	2.43	0.6
Dy	2.68	4.39	2.25	4.05	14.12	11.63	2.52	13.98	5.21	10.17	4.9	2.13	14.38	3.84
Ho	0.53	0.87	0.45	0.87	3.01	2.43	0.49	2.9	0.98	2.07	0.99	0.41	2.85	0.79
Er	1.38	2.31	1.27	2.73	8.98	6.77	1.29	7.87	2.56	5.6	2.78	1.08	7.65	2.09
Yb	1.48	2.19	1.73	3.59	9.3	6.73	1.57	7.49	2.5	5.26	2.8	1.27	7.33	2.19
Lu	0.21	0.33	0.27	0.57	1.66	1.16	0.25	1.29	0.39	0.91	0.44	0.18	1.29	0.33
Hf	3.35	2.5	4.48	6.99	13.1	7.11	4.54	8.59	3.36	6.02	4.9	4.33	8.53	4.32
Ta	0.74	0.27	1.7	1.84	3.06	1.3	1.33	2.03	0.79	1.08	1.38	0.85	1.75	1.15
Pb	4.93	41.49	7.66	11.98	40.4	28.05	15.81	111.4	8.3	42.74	12.9	8.21	14.85	4.58
Bi	0.16	0.21	0.14	0.49	0.81	0.08	0.13	0.18	0.15	0.02	1.01	0.08	0.08	0.23
Th	10.34	1.16	14.89	18.71	42.05	13.89	14.43	23.31	15.75	9.72	20.71	12.63	18.83	17.05
U	2.85	0.17	1.89	4.51	8.6	5.68	1.93	9.62	9.77	3.87	5.73	2.42	7.87	4.27

sample no	2009378020	2009378021	2009378023	2009378024	2009378025	2009378026	2009378027	2009378028	2009378029	2009378030	2009378031	2009378032	2009378033	2009378034
hole	ETM5A 1	ETM5A 1	ETM5A 1	BWM1A 1	BWM1A 1	BWM1A 1	SPH 1	SPH 1	SPH 1	SPH 1	SPH 1	SPH 1	SPH 1	SPH 1
lithology	Altered metasediment	Altered metasediment	Altered metasediment	Altered metasediment	Altered metasediment	Altered metasediment	Calc-silicate	Calc-silicate	Calc-silicate	Calc-silicate	Calc-silicate	Calc-silicate	Calc-silicate	Calc-silicate
Depth from	484.6	514.6	534.5	401.0	418.8	474.4	414.0	435.1	445.0	464.5	495.3	613.0	475.1	590.4
Depth to	484.9	515.0	534.9	401.2	419.1	474.8	418.9	435.3	445.5	465.0	495.8	613.4	480.0	590.9
SiO2	50.56	58.60	68.81	54.38	54.27	54.80	53.57	53.94	53.43	53.16	53.97	54.76	52.79	41.01
TiO2	0.43	0.63	0.52	0.43	0.59	0.74	0.71	0.50	0.48	0.60	0.60	0.53	0.60	1.13
Al2O3	10.37	16.29	14.63	15.25	16.08	16.37	11.14	11.44	14.50	12.18	11.90	13.00	8.70	13.77
FeO	1.00	1.00	0.30	1.65	2.72	2.34	5.87	6.17	4.42	6.71	6.69	3.91	9.93	3.73
Fe2O3	3.15	2.76	1.97	3.71	5.05	3.60	3.46	2.23	1.71	3.54	4.03	3.62	3.90	9.18
MnO	0.38	0.07	0.05	0.16	0.09	0.18	0.88	0.97	0.70	1.22	1.15	1.10	1.66	0.53
MgO	1.41	0.98	0.89	1.19	1.90	3.45	2.69	3.57	2.72	1.90	1.68	1.87	2.10	2.32
CaO	14.59	2.90	1.03	4.79	2.78	1.98	15.12	14.33	13.53	14.02	14.76	12.57	16.54	22.73
Na2O	2.31	3.50	5.23	4.18	3.87	2.18	4.58	4.48	5.60	3.84	4.51	5.21	3.97	0.89
K2O	5.57	8.76	4.45	6.88	7.35	9.26	0.31	0.72	0.61	1.75	0.77	1.52	0.18	0.03
P2O5	0.12	0.18	0.11	0.15	0.17	0.19	0.70	0.28	0.39	0.05	0.04	0.27	0.07	0.16
SO3	0.02	0.01	0.01	0.10	0.15	0.01	0.32	0.01	0.03	0.01	0.05	0.14	0.07	<0.01
F	<50	273	366	334	921	939	585	69	301	<50	<50	85	<50	528
Be	4	1.8	2.4	4.6	5.7	5.2	3.8	5	5.1	3	3.1	3.7	3	3.1
Sc	9.6	13.4	9.8	13.6	13.7	27.4	15.1	14.5	15.3	10.1	10.3	11.9	11.6	19
V	40	56	43	45	71	118	28	21	16	13	17	22	16	110
Cr	37	67	53	46	76	94	43	50	51	51	50	46	47	95
Ni	15	18	14	18	32	64	15	20	17	5	6	11	6	4
Cu	3	21	1	53	31	1	33	<1	1	2	3	3	2	3
Zn	19	29	10	56	31	103	829	851	731	612	789	1044	1104	83
Ga	12.3	13.2	18	20.3	17.8	25.9	14.2	12.1	16.5	14.3	13.5	15.7	10.8	32.1
Ge	2	0.7	1.2	0.8	1.4	1.5	1.3	1.1	0.7	1	1.2	0.8	1.3	2.1
As	8.9	9.7	1.7	15.4	11.8	10.9	18.6	9.3	13.2	1.7	12.7	7.7	3.3	2.1
Rb	176.4	264.1	131.9	287.9	328.4	441.3	9.6	19.2	15.4	58.4	32.3	60.9	5.2	0.5
Sr	56.6	59.6	33.1	78.5	153.8	129.2	194.1	335.1	374.8	311.4	293.9	196.6	139.7	557.5
Y	28	24.5	33.3	26	18.3	22.7	27.6	8.4	8.1	10.7	9.4	14.7	14.2	35.3
Zr	141.7	151.9	160.1	118.7	126.3	144.7	313.2	140.5	243.5	138.8	197.8	171.3	239	154.6
Nb	11.9	15.7	14.4	10.8	14.4	20	23.8	17	16.8	22.7	23.8	20.7	21.6	19.1
Mo	0.9	2.2	1.3	2.4	2.9	<0.3	1.9	0.8	0.5	1	0.9	1.1	0.6	2.5
Ag	<0.6	<0.6	<0.6	<0.6	<0.6	<0.6	<0.6	<0.6	<0.6	<0.6	<0.6	<0.6	<0.6	<0.6
Cd	<0.02	<0.02	<0.02	<0.02	<0.02	<0.02	1	0.25	0.3	0.34	1.33	1.12	1.47	<0.02
Sn	2	3.2	3.6	9.9	6.5	5.8	4.1	2.4	2.4	3.1	3.5	3.2	3.4	27.3
Sb	1.7	<0.8	<0.8	3.7	3.1	3.1	<0.8	<0.8	<0.8	1	1	<0.8	<0.8	<0.8
Cs	0.56	1.03	1.19	2.44	4.36	3.38	0.08	0.63	1.06	0.17	0.1	0.1	0.07	<0.03
Ba	795	1727	688.4	1662	2245	3367	117.8	341.9	254.5	858.8	326.4	968.2	46.1	7.4
La	32.48	20.35	20.71	57.29	153.5	74.63	191.5	65.62	137.1	30.44	28.47	64.81	35.96	50.87
Ce	63.35	44.77	40.54	107.2	252.6	139.6	286.6	101.3	200.3	59.18	61.09	101.5	71.22	86.27
Pr	7.08	5.76	4.58	11.21	24.13	15.58	24.27	8.75	16.28	5.94	6.39	9.28	7.38	9.29
Nd	26.16	23.48	17.28	35.64	69.71	54.55	62.88	22.73	38.53	16.79	19	25.82	21.44	31.59
Sm	4.89	5.31	3.26	5.29	7.38	9.04	6.74	2.26	2.96	1.76	2.09	3.14	2.56	5.58
Eu	0.757	0.826	0.544	0.785	1.221	1.456	0.924	0.283	0.367	0.259	0.267	0.416	0.348	1.41
Gd	4.35	4.81	4.16	4.31	4.6	5.67	4.78	1.71	1.72	1.44	1.44	2.3	1.95	5.35
Tb	0.68	0.73	0.81	0.66	0.58	0.71	0.73	0.21	0.19	0.18	0.17	0.31	0.29	0.85
Dy	4.02	4.39	5.44	4.21	3.31	3.74	4.41	1.55	1.33	1.54	1.38	2.25	2.06	5.52
Ho	0.83	0.83	1.12	0.85	0.59	0.75	0.92	0.29	0.27	0.33	0.3	0.47	0.46	1.15
Er	2.01	2.2	2.99	2.11	1.51	2.09	2.64	0.7	0.66	0.9	0.8	1.27	1.28	3.14
Yb	2.03	2.1	2.76	2.01	1.48	2.26	2.69	0.91	0.78	1.06	1.04	1.44	1.53	2.96
Lu	0.33	0.33	0.41	0.31	0.23	0.36	0.45	0.14	0.1	0.15	0.16	0.22	0.27	0.49
Hf	3.88	4.23	4.44	3.2	3.54	4.05	6.49	3.7	5.24	4.04	5.46	4.5	6.06	4.32
Ta	0.86	1.24	1.19	0.81	1.16	1.59	0.91	1.07	0.78	1.29	1.22	0.94	0.99	1.02
Pb	6.73	21.73	1.69	11.83	8.5	6.97	11.31	9.87	15.64	6.65	14.61	10.93	6.99	13.71
Bi	0.1	0.24	0.03	0.11	0.52	0.09	0.46	0.3	0.34	0.52	4.43	0.47	0.75	6.39
Th	13.73	19.88	15.37	12.26	20.65	23.67	109.6	28.25	77.41	5.11	3.75	18.37	5.81	3.69
U	3.06	5.21	2.07	5.57	8.59	6.71	17.1	5.31	10.78	2.94	2.69	5.06	7.01	9.54

sample no	2009378035	2009378036	2009378038	2009378039	2009378040
hole	SPH 1	SPH 1	BRD 012	BRD 012	BRD 013
lithology	Calc-silicate	Calc-silicate	Granite	Granite	Granite
Depth from	603.2	601.0	482.0	436.0	474.0
Depth to	603.7	601.5	488.0	440.0	474.5
SiO2	54.45	54.76	73.16	73.36	68.88
TiO2	0.50	0.51	0.21	0.21	0.32
Al2O3	12.30	11.63	12.24	12.27	13.71
FeO	5.29	5.27	1.63	1.80	1.85
Fe2O3	3.92	2.61	1.08	1.04	1.74
MnO	1.03	1.03	0.11	0.09	0.09
MgO	2.77	3.08	0.19	0.17	0.27
CaO	14.07	13.99	0.57	0.60	0.81
Na2O	4.99	4.20	2.46	2.39	3.10
K2O	0.61	1.71	6.04	5.93	5.92
P2O5	0.28	0.11	0.03	0.03	0.05
SO3	0.28	0.06	0.02	0.01	0.04
F	192	<50	3159	3226	2352
Be	3.9	4.7	6.1	6.5	5.4
Sc	11.6	13.2	16.7	17.7	17.6
V	19	22	7	8	10
Cr	45	47	1	2	2
Ni	21	22	<1	<1	<1
Cu	6	1	6	8	6
Zn	2072	766	92	65	276
Ga	19.3	13.2	26.1	25	27.4
Ge	1	1	1.9	1.7	1.7
As	6.9	5	19.4	33.3	27.5
Rb	13.4	75.4	359.3	354.9	333.1
Sr	372.3	249.2	22.2	18	56.7
Y	12.8	7.3	115.3	120.5	99.4
Zr	154	172.3	313.4	301.8	493.1
Nb	18	19.5	34.7	34.4	37
Mo	0.9	1.2	2.6	4	5.5
Ag	<0.6	<0.6	<0.6	<0.6	<0.6
Cd	3.08	0.66	<0.02	<0.02	0.46
Sn	3	2.7	6.3	8.3	7.2
Sb	0.8	0.9	1.7	2.4	1.6
Cs	0.06	0.14	3.02	2.57	3.26
Ba	123.6	834.2	746.3	726.3	1007
La	66.72	42.81	112.7	116.1	94.13
Ce	104.9	72.99	229.8	237.3	192.5
Pr	9.59	6.86	26.86	27.8	22.81
Nd	26.11	18.52	97.89	101.6	84.39
Sm	2.94	1.74	20.77	21.37	17.48
Eu	0.417	0.208	1.228	1.257	2.235
Gd	2.2	1.23	18.04	18.88	16.16
Tb	0.29	0.13	3.21	3.31	2.77
Dy	1.94	1.18	19.14	19.6	16.62
Ho	0.43	0.22	3.87	4.03	3.33
Er	1.14	0.61	10.62	11.02	9.23
Yb	1.25	0.78	10.21	10.85	8.74
Lu	0.22	0.12	1.79	1.88	1.52
Hf	4.07	4.63	10.04	9.89	13.72
Ta	1.03	1.03	2.79	2.88	2.77
Pb	14.6	12.37	71.04	23.36	117.7
Bi	0.71	0.75	0.64	0.96	0.36
Th	19.47	11.81	52.75	55.14	40.04
U	6.43	4.38	15.87	16.49	12.54